

For Reference

NOT TO BE TAKEN FROM THIS ROOM

Ex libris
UNIVERSITATIS
ALBERTAENSIS



THE UNIVERSITY OF ALBERTA

GEOCHEMISTRY OF
SOME OCEAN-FLOOR BASALTS
OF CENTRAL B.C.

by

BARTON M. HALL-BEYER



A THESIS

SUBMITTED TO THE FACULTY OF GRADUATE STUDIES AND RESEARCH
IN PARTIAL FULFILMENT OF THE REQUIREMENTS FOR THE DEGREE
OF MASTER OF SCIENCE

DEPARTMENT OF GEOLOGY

EDMONTON, ALBERTA

FALL, 1976

ABSTRACT

The basaltic rocks of the Slide Mountain Group have been gathered from three field areas in central British Columbia. In the field a number of rock types are found, but their bulk chemistry is more uniform than this would indicate. Several major and trace element chemical screens establish these rocks as ocean-floor basalts, unassociated with the generation of island arc material. The great majority of the rocks are tholeiites, but a significant number are komatiites. Upper Palaeozoic in age, the komatiites are substantially younger than any others so far described. Both the komatiites and the ocean-floor tholeiites are the first reported from the Cordillera. Analyses of 30 elements provide data that are lacking for Cordilleran greenstones, particularly in the case of the trace elements. These data also perform an interpretive function in establishing the suite as being of ocean-floor origin. This is particularly useful because the rocks have been metamorphosed.

This study makes the following interpretations as a first approximation of the tectono-chemical genesis of the suite. The tholeiites have been derived by the fractionation of a garnet peridotite and are largely similar to other ocean-floor tholeiites. The komatiites have been derived by the fractionation of an orthopyroxene-clinopyroxene mix which contained little olivine. This may be the result of a very rapid rise of mantle material from a depth greater than that which gives rise to the mass of oceanic tholeiites.

ACKNOWLEDGEMENTS

The people who have influenced this study the most are:

- 1) Dr Richard LAMBERT, University of Alberta, who provided inspiration, guidance, and financial support (from his National Research Council grants).
- 2) Dr Halfdan BAADSGAARD, University of Alberta, who was of great help in setting up the atomic absorption procedure.
- 3) Dr Roger LAURENT, Université Laval, who first introduced me to the excitement of greenstones.
- 4) Dr J Grenville HOLLAND, Durham University, who is responsible for the x-ray analyses.
- 5) Randolph HALL, metallurgist, who analysed for carbon by combustion.
- 6) Mryka HALL-BEYER, companion and fellow petrologist.

TABLE OF CONTENTS

	<u>Page</u>
INTRODUCTION	1
Objectives	1
Geologic setting	1
Geography	1
FIELD DESCRIPTION	5
Clearwater Map Area	5
MacKay River Map Area	8
Barkerville Map Area	11
PETROLOGY	14
Introduction	14
Pyroxenite	14
Amphibolite	14
Fine-grained basalt	21
Porphyritic basalt	22
Quenched basalt	24
Pillowed basalt	24
Chlorite-Actinolite schists	27
Discussion	28
PETROCHEMISTRY - MAJOR ELEMENTS	30
Tholeiites	30
Komatiites	48

PETROCHEMISTRY - TRACE ELEMENTS	57
Introduction	57
Yttrium and Niobium	57
Zirconium	62
Lithium	69
Rubidium-Strontium-Barium	69
Transition Metals	71
Co-Ni-Cu-Zn	72
Molybdenum and Lead	73
CONCLUSION	75
REFERENCES CITED	78
APPENDIX 1: ANALYTICAL PROCEDURES	82
Atomic Absorption Spectrophotometry	82
Permanganimetric Titration of Ferrous Iron	85
Determination of Carbonate	87
Electron Microprobe	88
X-ray Fluorescence	89
APPENDIX 2: CIPW NORMS AND OTHER VALUES	90
APPENDIX 3: COMPARATIVE TRACE ELEMENT ANALYSES	99
APPENDIX 4: COMPARATIVE CHEMISTRY	100

LIST OF TABLES

<u>Table</u>	<u>Description</u>	<u>Page</u>
1A-1F	Tholeiite / High-Zr Suite	32-37
2A-2F	Tholeiite / Average-Zr Suite	38-43
3A-3C	Komatiite / Low-Zr Suite	49-51
A1	Analysed Standards	83
A2a-2c	CIPW Norms of High-Zr Suite	91-93
A3a-3c	CIPW Norms of Average-Zr Suite	94-96
A4a-4b	CIPW Norms of Low-Zr Suite	97-98
A5	Comparative Tholeiitic Analyses	101
A6a-6b	Comparative Komatiitic Analyses	102-103

LIST OF FIGURES

<u>Figure</u>	<u>Description</u>	<u>Page</u>
1	Location Map, British Columbia	2
2	Regional Geology of Central British Columbia	3
3	Clearwater Map Area	7
4	Diagrammatic Columnar Section	9
5	MacKay River Map Area	10
6	Barkerville Map Area	10
7	$[Al]^4$ vs Na+K	18
8	Mg vs $[Al]^4$	19
9	AFM Diagram	31
10	$TiO_2 - K_2O - P_2O_5$ Diagram	45
11	Normative Plagioclase-Olivine-Diopside Diagram	47
12	$MgO - Al_2O_3 - CaO$ Diagram	54
13	Trace Element Histograms	58
14	Y vs Thornton-Tuttle Differentiation Index	59
15	CaO vs Y	61
16	Nb vs Y	63
17	Zr vs Thornton-Tuttle Differentiation Index	64
18	Zr vs Na_2O	65
19	Zr vs TiO_2	66
20	Ti/100 - Y x3 - Zr Diagram	68
21	Li vs MgO	70
22	Ni vs MgO	74

LIST OF PHOTOGRAPHIC PLATES

<u>Plate</u>	<u>Description</u>	<u>Page</u>
1	Pillow Lavas at Station [5550]	6
2	Pillow Lavas at Station [5551]	6
3	Pillow Lavas at Station [5556]	12
4	Contact between the Slide Mountain Group chlorite schists and the Kaza Group gneisses	12
5	Diopside from Pyroxenite at Station [5723]	16
6	Brown Hornblende rimmed by Blue-Green Hornblende and Actinolite	16
7	Fine-grained Basalt	23
8	Porphyritic Basalt	23
9	Quench Texture in the Slide Mountain Group	25
10	Quench Texture in the Slide Mountain Group	25
11	Quench Texture in Basalt from Leg 37 of the Deep Sea Drilling Project	26
12	Devitrified Glass in a Pillow Lava from Station [5550]	26

INTRODUCTION:

Objectives:

This study has two objectives, inspired by MONGER (1972) in his contribution to the Carleton University symposium on the ancient oceanic lithosphere in October 1970. They are:

- a) A detailed petrochemical study which might be used to refine the plate tectonic model for the Cordillera.
- b) Supporting petrographic and field studies.

Geologic setting:

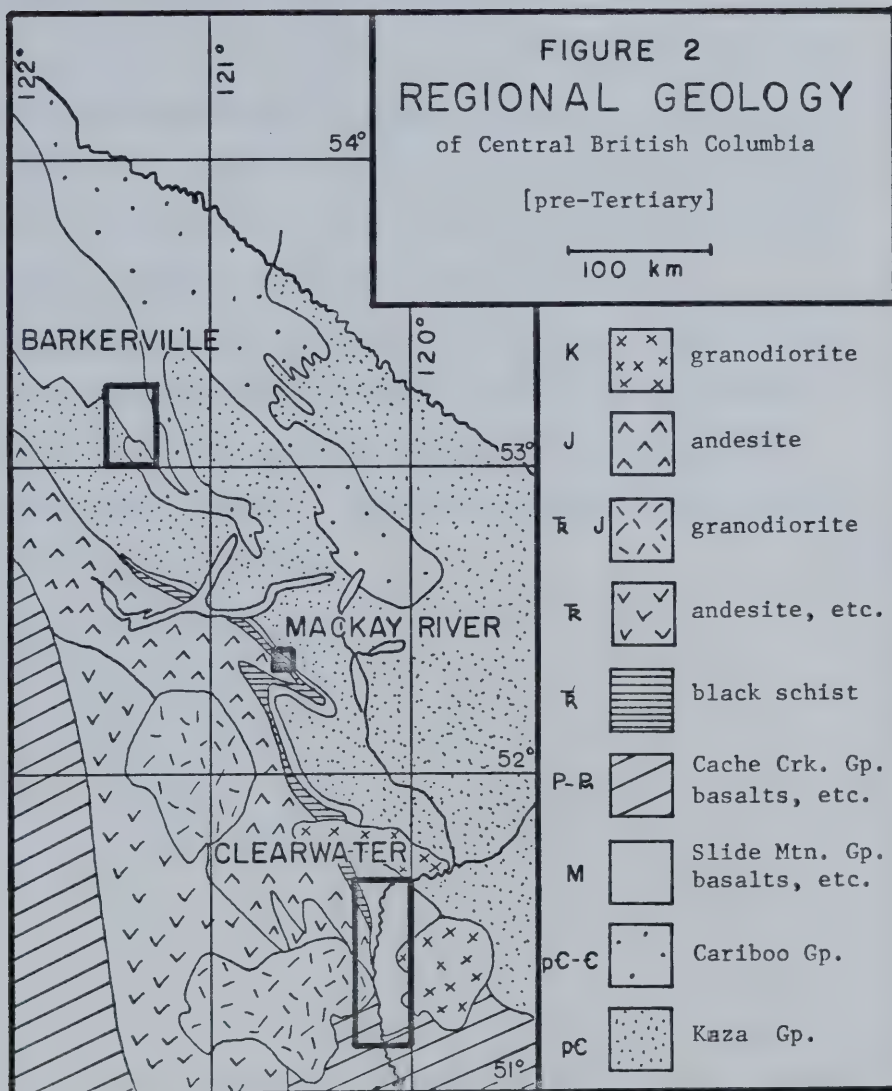
Located in south central British Columbia at the southern end of the Cariboo Mountains (see Figure 1), the Slide Mountain Group forms a thin unit extending some 700 km southeastward from the Prince George area (see Figure 2). The Group is on the western flank of the Omineca Crystalline Belt, and rocks of the Cache Creek Group are possibly equivalent.

Because of its rugged terrain, the Omineca Crystalline Belt has been little studied, but it is believed to have been deposited on the western margin of the Cordilleran miogeosyncline in the late Proterozoic (CAMPBELL, 1971). The basalts, etc. of the Slide Mountain Group were emplaced in the late Palaeozoic (CAMPBELL and TIPPER, 1971) and from the Triassic onward siltstones, black schists, and andesitic material were deposited above the Slide Mountain Group. The whole region was later intruded by numerous granodiorite plugs.

Geography:

With the exception of the prominent cliffs to the east of the North Thompson River in the Clearwater Map Area, most of the Slide Mountain Group is poorly exposed. The best available areas are





road-cuts along the Yellowhead highway between Clearwater and Little Fort because the cliffs to the east of the river are virtually inaccessible, but these road-cuts are limited in extent. In the MacKay River Map Area, exposure is quite poor, as the rock unit is narrow and the undergrowth dense. Exposure in the Barkerville Map Area is little better. In both the Barkerville Map Area and the MacKay River Map Area, the exposure is poor enough to limit seriously the quality of the study that could be done.

Weathering of the outcrops was not a serious problem. Many of the outcrops were the road-cuts created by the Yellowhead Highway, and the rocks there are very fresh, except in badly fractured areas. Elsewhere, weathering is usually much less than 5 mm and was easily trimmed.

FIELD DESCRIPTION:

Clearwater Map Area:

Approximately 3000 metres of the Slide Mountain Group were studied in the southernmost exposure of the group, from Barrière to Clearwater (see Figure 3). South of Little Fort the rock is rather uniform, massive, and very fine-grained greenstone. It is often fractured and contains the infrequent chert bed. Some schistosity and minor faulting are also present.

The rocks frequently display a rather shiny green aspect, and can be mistaken in the field for serpentinites. The similarity is heightened by a certain amount of veining along the fractures. In other localities the fracture pattern gives the impression of pillows, which confusion is rendered more effective by the presence of scattered *bona fide* pillows near the top of the greenstone unit.

Except for one band of what is believed to be pillow breccia [5614],^T the massive greenstone is approximately 1200 metres thick. In the eastern part of the field area much of the rock is altered by a large granodiorite body, and this altered rock was sampled in two places only, [5605] and [5765].

In the central part of the field area, [5550], [5551], and [5556], there occurs a 200 metre band of pillow lavas of unknown extent. As shown in Plates 1, 2, and 3, the pillows are well-shaped buns, of normal orientation. Unfortunately, this band could not be traced across the river, so the dimensions of the flow

^T the designation [XXXX] refers to both sample numbers and locations



PLATE 1

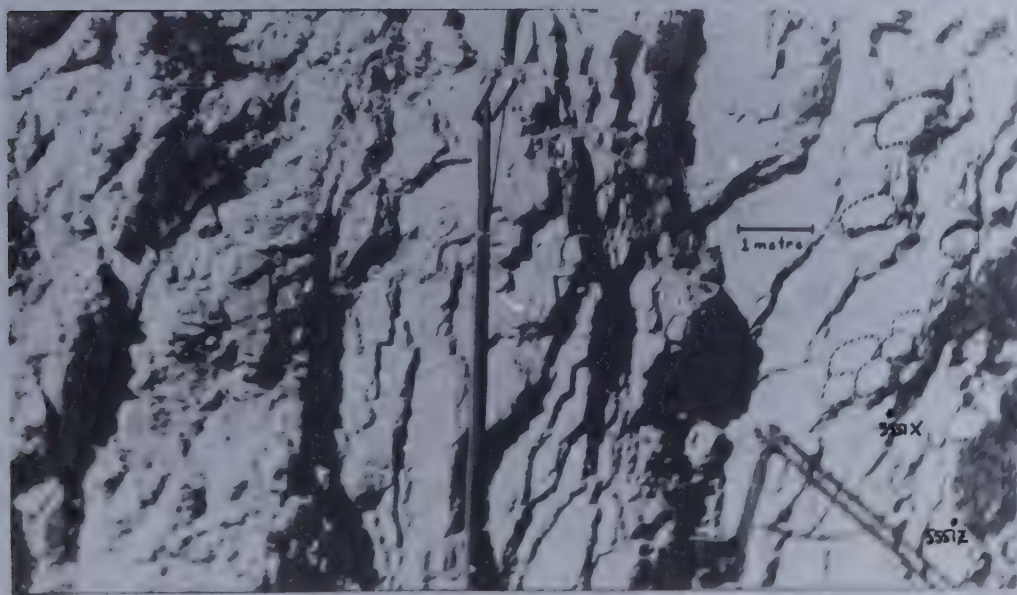
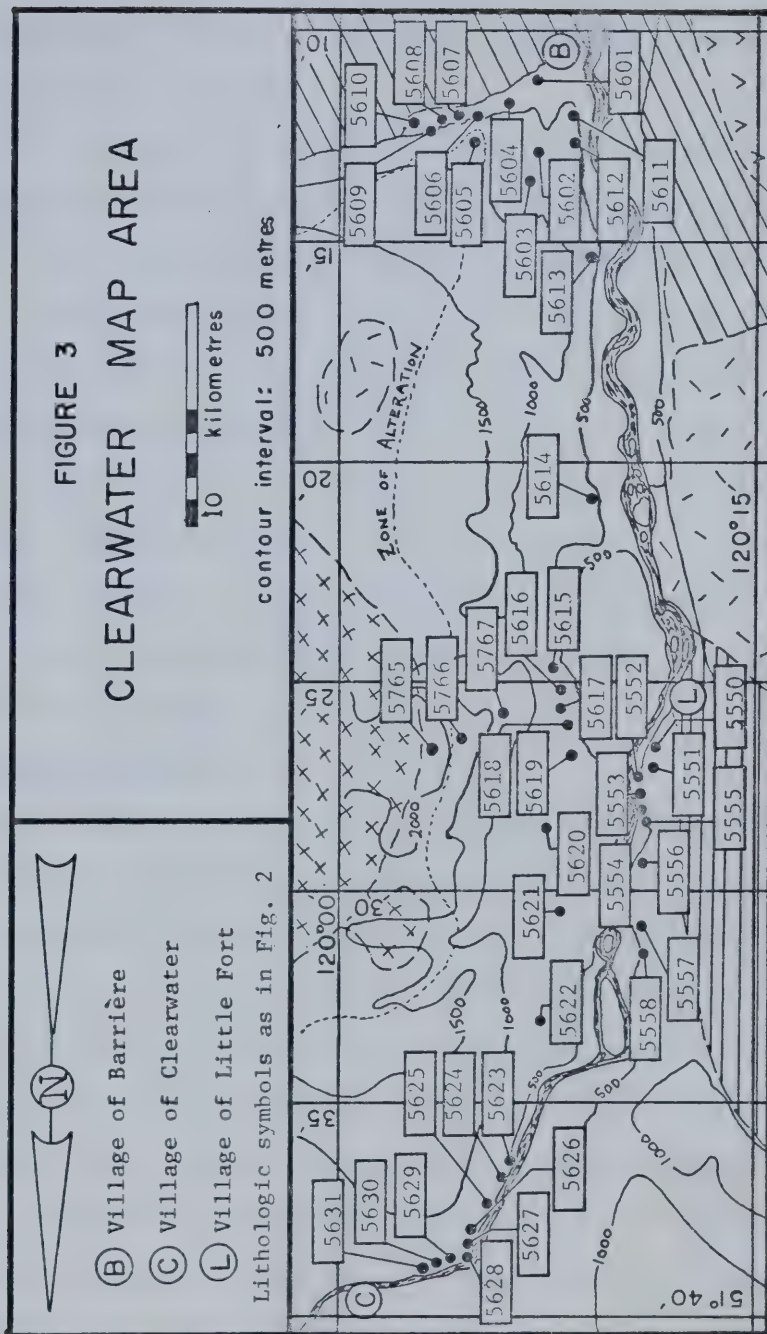


PLATE 2



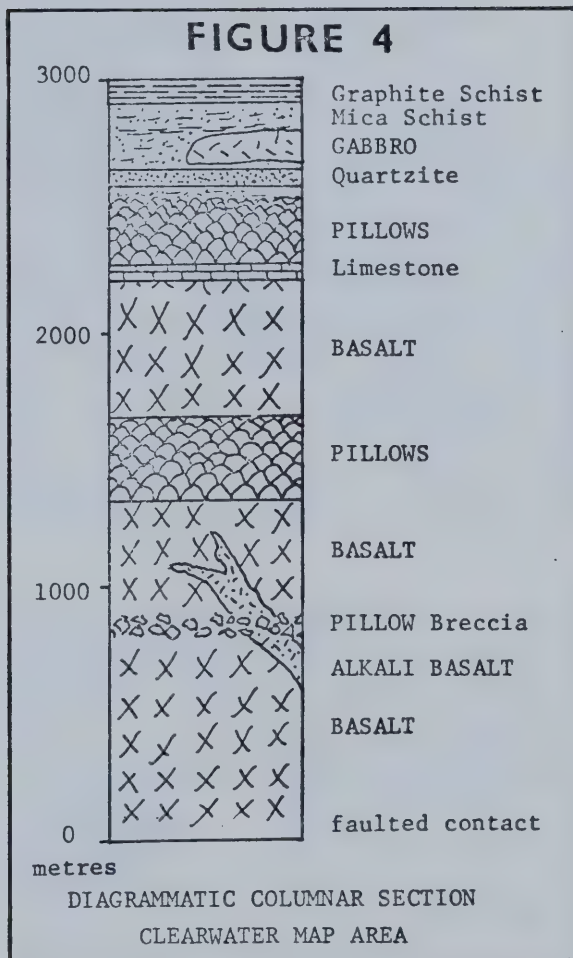
are indeterminate. These pillows are overlain to the north by another 500 metres of massive, fine-grained greenstone, which is often quite badly fractured.

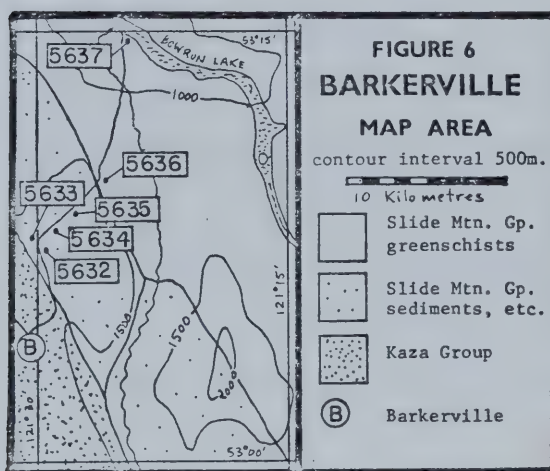
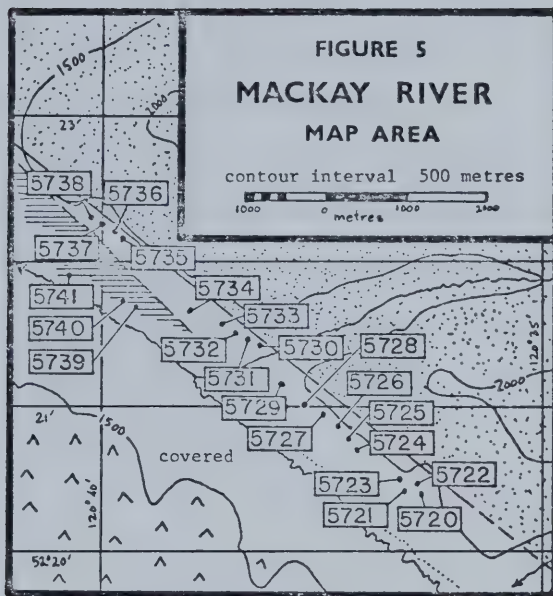
At the northern limit of the field area, near Clearwater, the sequence becomes much more varied, and includes many sedimentary members. One hundred metres of limestone are overlain by 200 metres of pillow lavas [5624]. Above this are mica schists [5625], massive quartzites up to two metres thick [5626], graphite schists [5626A], and immature partially volcanic sediments up to 100 metres thick. Graphite schist is the dominant lithology for the next 200 metres, [5628] and [5629], but it is interrupted by a 30 metre gabbro sill, [5630], and a band of quartzite and mica schist, [5631]. The section ends against another granodiorite body, and is summarised in Figure 4.

MacKay River Map Area:

In the MacKay River Map Area (see Figure 5) the exposure of rock is so poor that it is barely acceptable for mapping purposes. The Slide Mountain Group in this area is very thin, and probably badly faulted. It is no more than about 400 metres thick, and it thins to a few tens of metres in the northern part of the map area. Most sample locations are only approximate, a result of heavy undergrowth which makes accurate location of field stations impossible.

The lithology is variable from a pyroxenite to a chlorite schist, but a very general division into coarse-grained, fine-grained and schistose rock types is possible in the field. The coarse-





grained rocks are nearly all amphibolites and occur only in the southern part of the field area; [5720], [5721], [5722], and [5724]. The pyroxenite is in the same area, [5723], and appears similar to the amphibolites except that it is less friable.

The fine-grained rock is represented by [5721A] and contains sufficient epidote to give the rock its characteristic apple-green colour. Field and hand specimen relationships suggest that this fine-grained rock was the country rock intruded by the coarse-grained phases. The exact intrusive relationships, however, could not be determined due to the poor exposure.

The great majority of the rock in the area is a shiny chlorite schist that is sometimes crenulated, sometimes not; sometimes banded, sometimes not; sometimes quartz-bearing, sometimes not; and sometimes feldspathic, sometimes not. The general impression received is that the metamorphic grade decreases towards the northwest, but this cannot be confirmed in the field. Plate 4 shows the contact of these chlorite schists with the Kaza Group schists and gneisses.

Here, as in the Clearwater Map Area, the Slide Mountain Group is overlain by graphite schists; [5739], [5740], and [5741]; though the quartzites noted in the Clearwater Map Area are not present.

Barkerville Map Area:

The greenstone lithology of the Slide Mountain Group was sampled in but one locality, [5636], to provide a link between the type area of the group and the two major field areas to the south. It is



PLATE 3

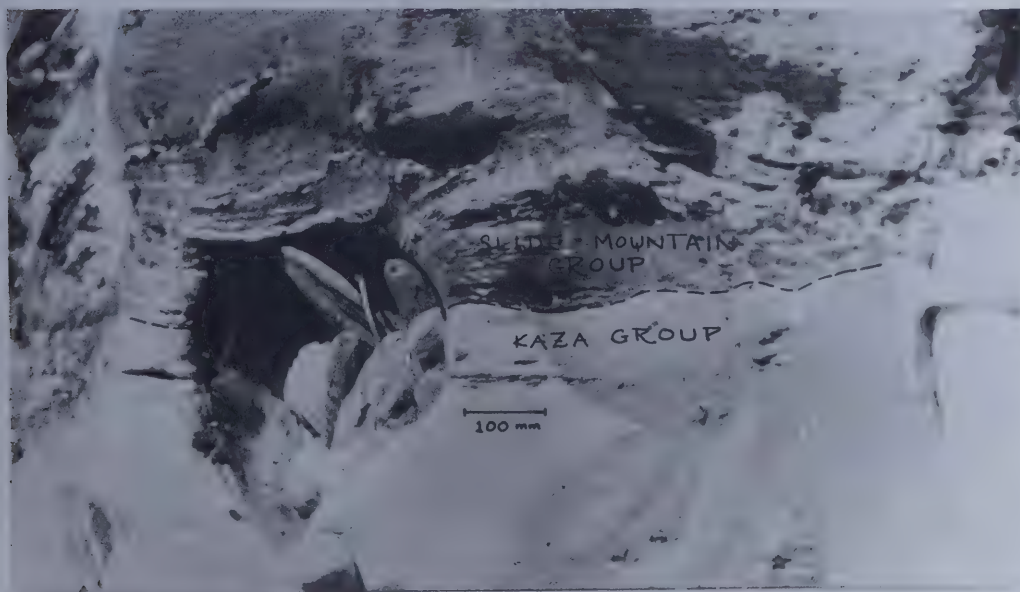


PLATE 4

worthy of note that in this area the greenstone occurs both as massive rock and as breccia. The breccia is subrounded, generally in fragments larger than 100 mm, and is suspended in a matrix of white chert which overlies the massive greenstone.

PETROLOGY:

Introduction:

Although this study is geochemical, the petrology of the rocks involved has proven to be of sufficient interest to be included as a separate section. The following discussions are offered not as a definitive petrographic study, but as an examination with microscope and microprobe which may function contrapuntally with the geochemical study and outline some problems for future consideration.

Pyroxenite:

Found only at [5723], this pyroxenite seems to be decidedly relict. Diopside (see Plate 5) is the predominant mineral and has the composition

Ca	Mg	Fe	Si	Al	O	*1
.98	.80	.19	1.92	.08	6	

Chlorite and actinolite rim many of the grains, as even in this rock the alteration progressing to amphibolite has begun. This is, without question, a primary plutonic pyroxenite which has somehow escaped almost entirely the process of hydrous amphibolitisation.

Amphibolite:

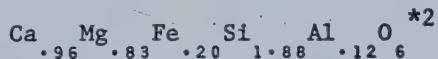
Confined to the southern portion of the MacKay River Map Area, the amphibolites are a series of rocks which have been produced by the hydration to varying degrees of the pyroxenite represented by [5723]. Their mineralogical complexity is best characterised by the amphiboles which make up the bulk of

*1 trace elements in mole percent

Sc 0.02; Ti 0.19; V 0.03; Cr 0.06; Mn 0.05; Co 0.04; Ni 0.01

these rocks.

In the samples containing pyroxenes, the common alteration is to actinolite, occurring in the less altered samples along grain boundaries and internal cracks. One analysed actinolite from [5724] was derived from a diopside of composition



and the actinolite composition



indicates considerable major element mobility, particularly Ca (out), alkalis (in), and Fe (in). However, it is notable that Mg, Al, and Si have remained in constant proportion.

Optically there is great variation in the amphiboles of all samples, ranging from pargasites (primary? brown hornblendes) to hornblende *sensu strictu* (both green and blue-green) and several generations of actinolite. In some samples the actinolite exists as large blades, overgrown with one or more generations of actinolite which appears on the basis of optical properties to be of approximately the same composition. In other samples, the actinolite is definitely prismatic, and in still others fibrous or acicular. Some slides display all these aspects.

Situations in which a core of brown hornblende is rimmed by green and/or blue-green hornblende, and then in turn by one or more varieties of actinolite are not uncommon (see Plate 6).

*2 trace elements in mole percent

Sc 0.02; Ti 0.11; V 0.04; Cr 0.06; Mn 0.04; Co 0.02; Ni 0.01

*3 trace elements in mole percent

Sc 0.01; Ti 0.11; V 0.04; Cr 0.06; Mn 0.04; Co 0.01; Ni 0.01

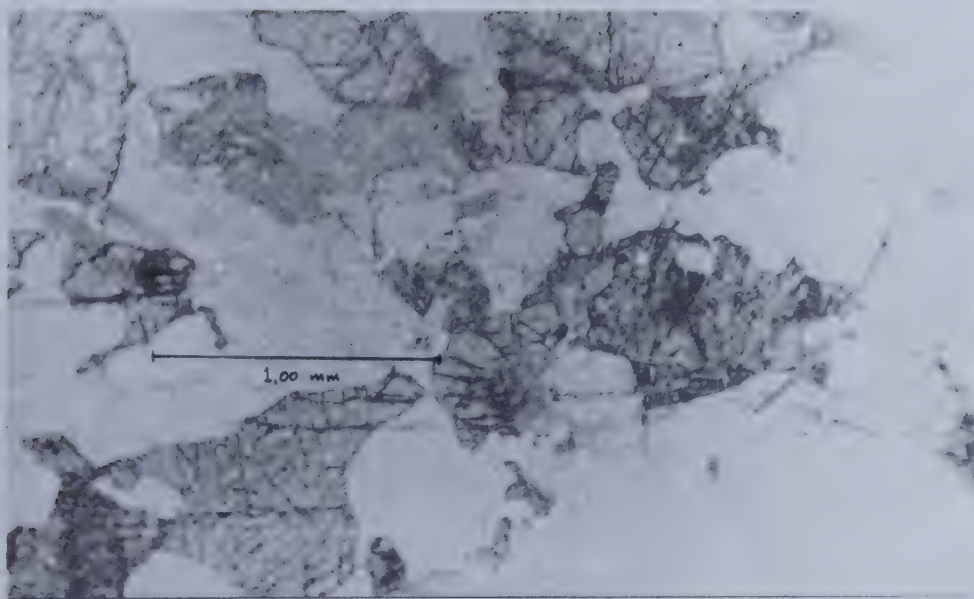


PLATE 5

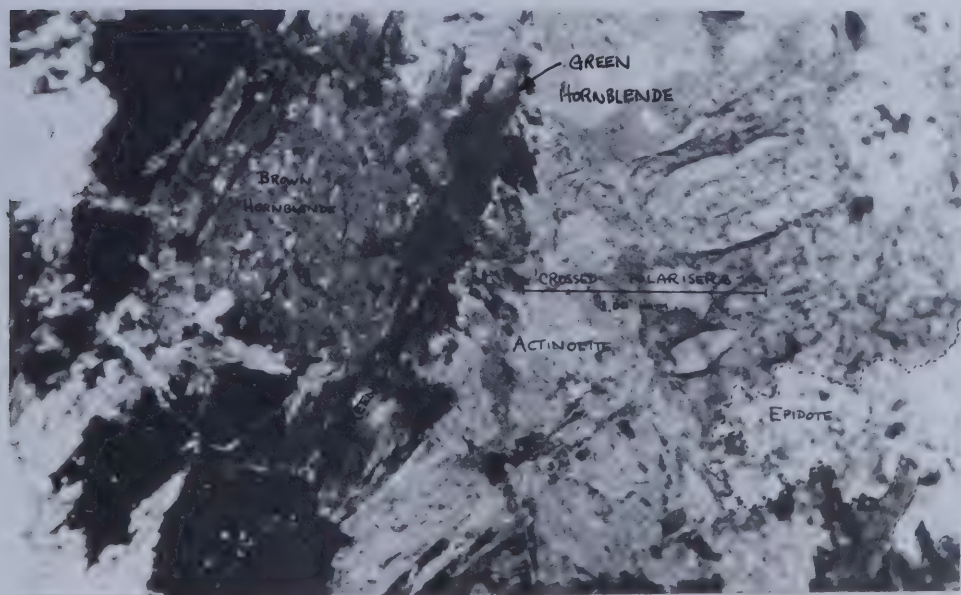


PLATE 6

Nor is the zoning pattern pyroxene/green hornblende/actinolite uncommon. However, nowhere was augite or diopside observed as the core of a grain which contains brown hornblende. This suggests that the brown hornblende may well be primary and cogenetic with the pyroxene. The almost complete lack of plagioclase in any of these rocks is certainly compatible with a primary aluminous and alkali basic mineral. The pargasites also contain significant amounts of Cl and a bit of F, both of which are lost on conversion to actinolite.

The chemical relationships of the various amphiboles are summarised in Figure 7 (after SPRINGER, 1974) and in Figure 8 (after SHIDO and MIYASHIRO, 1959) which include other analysed amphiboles from this study. SPRINGER (1974) used the plot on which Figure 7 is based to determine from actinolite compositions whether or not a given metamorphic rock had contained orthopyroxene. Of the analyses actinolites, most fall in the orthopyroxene bearing field, but the location of points from [5721A] suggests that the protolith was not a two-pyroxene rock, unlike the others in the amphibolite series. The origin of [5721A] is uncertain, but field relationships lead one to believe that it was intruded by the actinolitic hornblendite of [5721]. The hypothesised absence of orthopyroxene suggests that [5721A] was not comagmatic with [5721].

The miscibility gap postulated by SHIDO and MIYASHIRO (1959) is well displayed in the amphiboles of this study, but the authors'

FIGURE 7

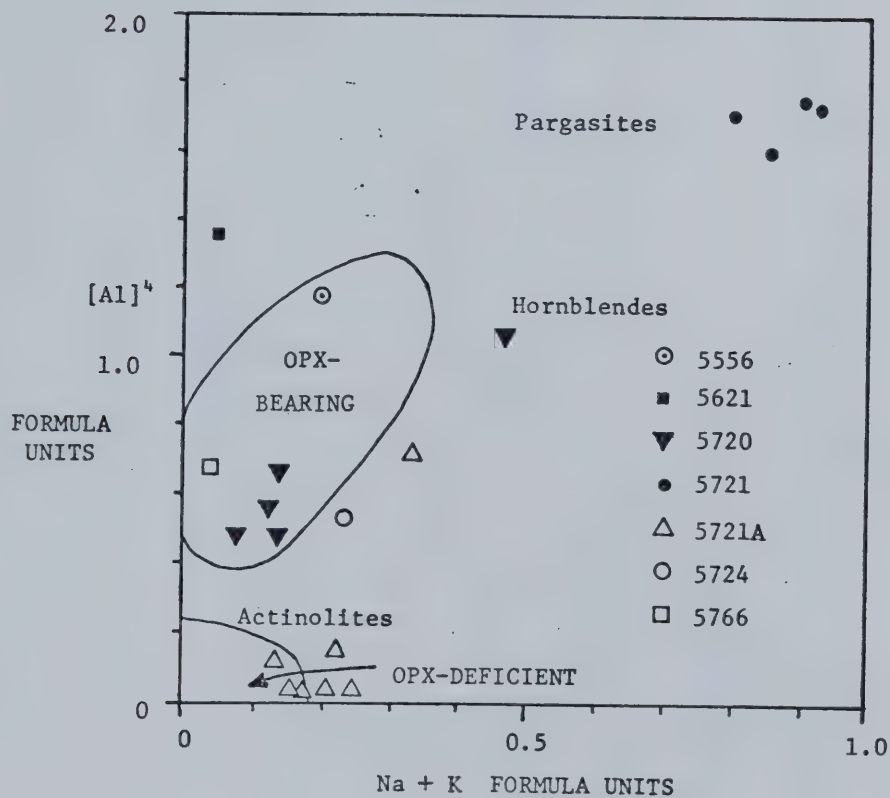
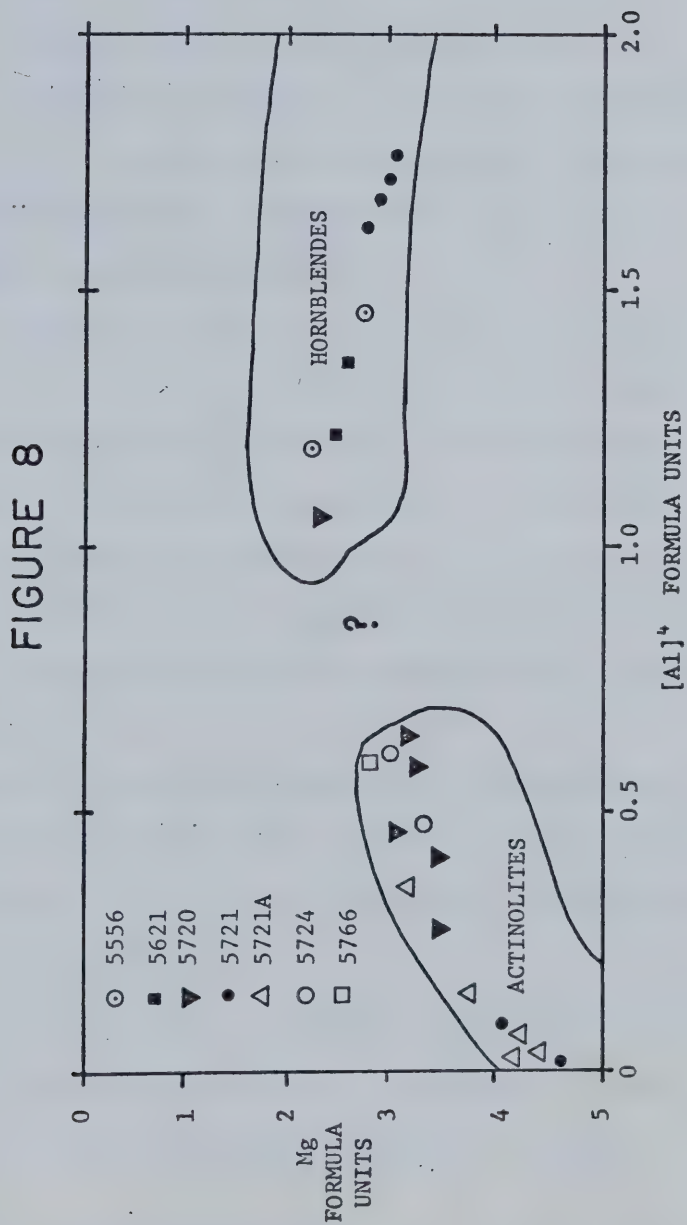
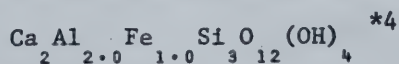
Figure 7: $[Al]^4$ vs $Na+K$

Figure 8: Mg vs $[Al]^4$ 

suggestion that the gap narrows with higher metamorphic grade and/or shifts towards lower [Al]⁴ could not be confirmed since the Slide Mountain Group is at low metamorphic grade in the areas studied. CAMPBELL (1971) reports a number of kyanite - staurolite grade amphibolites in the Slide Mountain Group to the south of the MacKay River Map Area, and this is not surprising given the steep and convoluted isograds there present. CAMPBELL's amphibolites would thus present a good opportunity to verify the thesis of SHIDO and MIYASHIRO (1959).

It has been impossible so far to confirm either the prograde or the retrograde metamorphism of the Slide Mountain Group amphibolites, but this preliminary study suggests a length and retrograde metamorphism of pyroxenite into amphibolite (actinolite). Later prograde, but here minor, metamorphism can account for the several generations of actinolite. CAMPBELL's higher grade rocks should be able to help clarify the chemical and metamorphic relations of the amphiboles.

The balance of the minerals usually consists of epidote and chlorite in roughly equal proportions. Epidote is uniformly very iron-rich, shown by both the deep green colour and the microprobe



It usually occurs as small blebs and chunks in what might be called a felted mass of actinolite and chlorite. A markedly different habit is present in some slides, epidote occurring as tabular

*4 trace elements in mole percent

Sc 0.03; Ti 0.02; V 0.10; Cr 0.04; Mn 0.02; Co 0.02; Ni 0.01

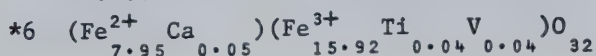
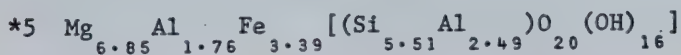
groups and aggregates of barrel-shaped crystals suggestive of prehnite. Negative optic sign and higher refractive index, however, indicate epidote, though the habit may be remnant from prehnite.

Chlorite is usually ripidolite ^{*5}, though alumina-poor compared to what might be expected. Some slides contain both clinoclhor and ripidolite, and this is easily detected by the colour difference under crossed polarisers. Most frequently it occurs as tabular to lath-like crystals forming a network in conjunction with actinolite. Whether it is a prograde product or a retrograde product is not known.

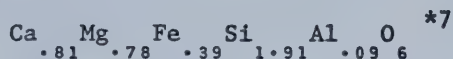
Minor components include magnetite ^{*6}, apatite, sphene, pyrite, chalcopyrite, carbonate, haematite, leucoxene, and various indeterminate alteration products.

Fine-grained basalt:

In thin section, these rocks display a decidedly subophytic texture, with plagioclase the dominant mineral (see Plate 7). Plagioclase consistently comprises about half of the rock, and usually exists as both laths and grains, the 1:1 proportion of which remains relatively constant from rock to rock. The laths are usually 0,50 mm long, while the equant grains are about 0,10 mm across. Several analyses show the plagioclase to be albite (An_{4-7}) which is in general agreement with optical determinations from the few polysynthetic twins present.



Augite is usually subhedral and more or less equant. It can, however, display lath-like aspects as though it had been broken. The size varies from 0,05 mm to 0,20 mm, but the equant grains are rarely larger than 0,10 mm. The analysed augite from [5621] is nearly twice as iron rich as the diopside of the amphibolites



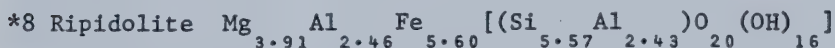
and comprises about thirty percent of most rocks. The remaining 15 - 25% groundmass consists of finely divided chlorite ^{*8}, actinolite pumpellyite, epidote ^{*9}, prehnite(?), clay ^{*10}, apatite, and opaques.

Porphyritic basalt:

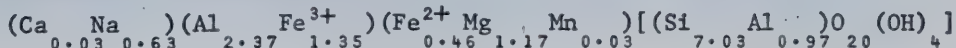
Characterised by augite phenocrysts up to 1,00 mm across (see Plate 8), this porphyritic variant of the fine-grained basalt displays a slightly different mineralogy. Plagioclase still comprises about half of the rock, but it is strongly sericitised. Some minor olivine is present, as is hornblende. The hornblende is usually interstitial, but sometimes occurs after augite. No pumpellyite or prehnite was found.

*7 trace elements in mole percent

Sc 0.00; Ti 0.36; V 0.05; Cr 0.02; Mn 0.10; Co 0.03; Ni 0.01



*10 Nontronitic montmorillonite



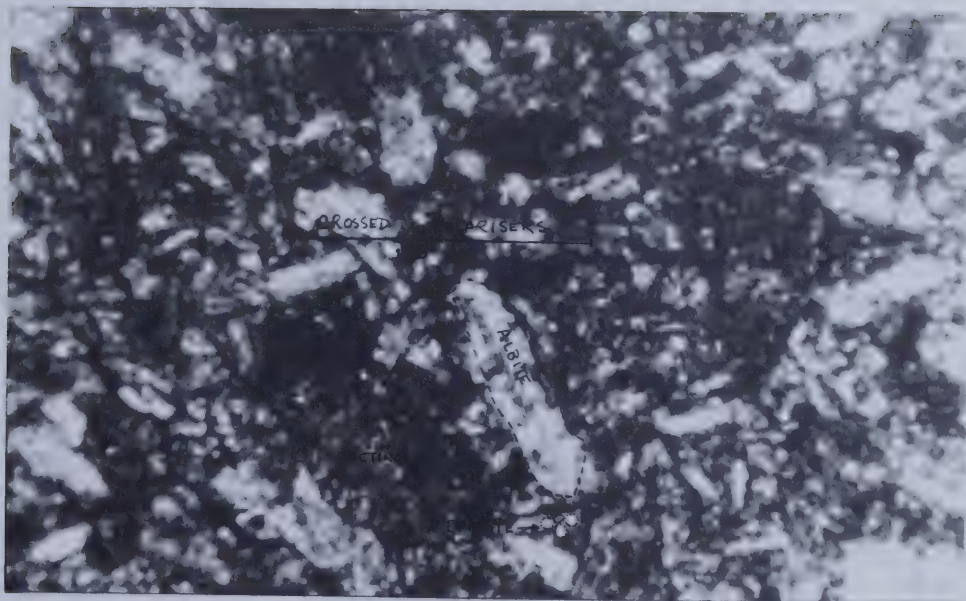


PLATE 7

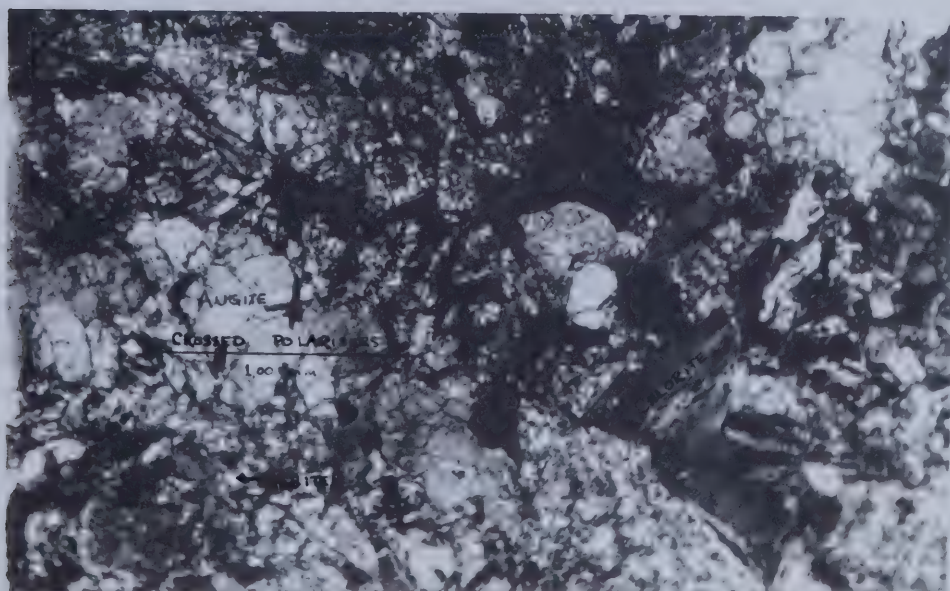


PLATE 8

Quenched basalt:

Texturally, these rocks are very similar to those from Leg 37 of the Deep Sea Drilling Project (see Plates 9, 10, and 11). Minor amounts of augite are visible, and some rocks have more phenocrysts than others. Plagioclase is prominent in radiating bundles, and while averaging 0,25 mm in length, can be twice that. The groundmass comprises one half of the total and includes actinolite, plagioclase, chlorite, pumpellyite(?), and minor quartz. Calcite and a zeolite(?) may also occur as vug fillings, and the zeolite(?) may comprise part of what is called plagioclase in the groundmass.

Pillowed basalt:

Two pillows nearly a metre across, [5550] and [5624], and one pillow 100 mm across, [5556], were studied to provide comparison to the more massive rocks. The pillow [5550] consists of mineralogically and texturally complex devitrified glass (see Plate 12). Identifiable minerals are plagioclase, chlorite, actinolite, augite, pumpellyite(?), and accessories. About 80% of the rock is 0,01 mm and smaller material consisting of the above minerals and much unidentifiable material.

The pillow [5624] again consists of a large percentage of devitrified glass, but contains enough larger material to exhibit quench texture. Much of the devitrified glass has been metamorphosed to chlorite, epidote, and actinolite (or/and pumpellyite), but included therein are a number of amygdaloids which display a

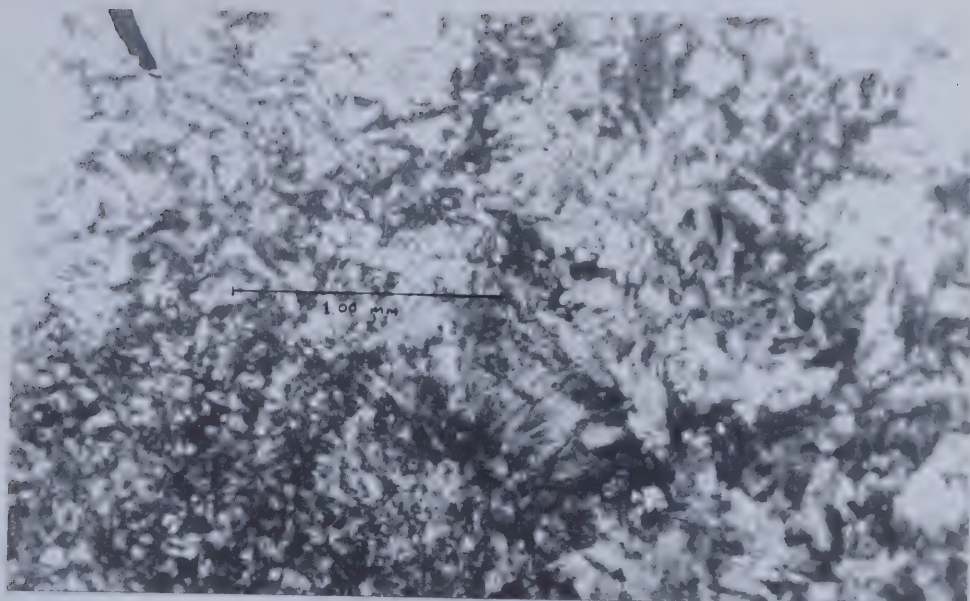


PLATE 9

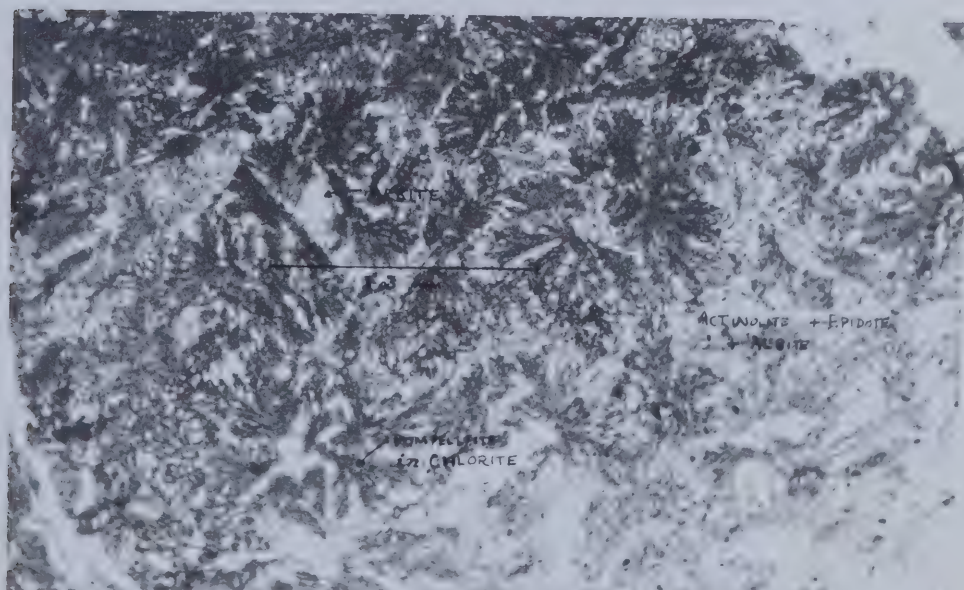


PLATE 10

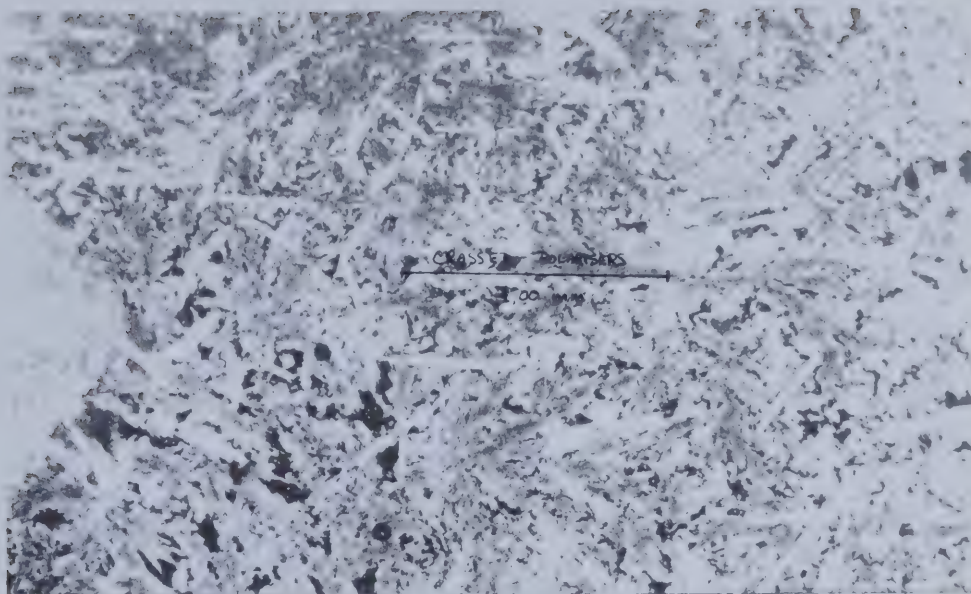


PLATE 11

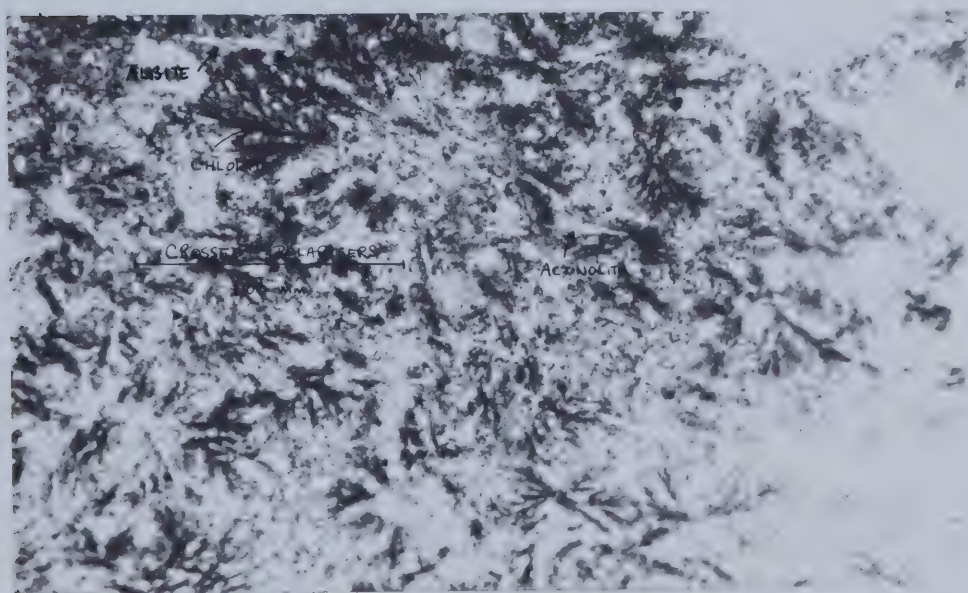


PLATE 12

zeolite type of structure which has since been metamorphosed to a mixture of zoisite, calcite, chalcedony, and quartz, with some pseudomorphs, possibly after prehnite.

The only pillow with even rudimentary structure is [5556] which consists of a 40 mm core, a 30 mm intermediate zone, and a 10 mm rind of devitrified glass. Thirty percent of the core consists of 0,08 mm fragments of augite ^{*11} which are often altered to actinolite. Plagioclase is present as 0,15 mm laths and as groundmass material for a total of about 40%. The balance is altered devitrified glass consisting of clays, zeolites, epidote, and actinolite.

The intermediate zone has radiating stringers of calcite in a matrix of devitrified glass similar to that of the core, but comprising 80% of the zone. Augite is absent, but quartz is present to a total of about 5%. The plagioclase is nearly identical to that of the core.

Chlorite-actinolite schists:

Highly varied, these greenstones form the bulk of the Slide Mountain Group in the MacKay River Map Area, and are found there only. In general, they tend towards the assemblage: chlorite-epidote-actinolite-plagioclase+quartz. Some of what is called actinolite may be pumpellyite, and the possible pumpellyite is present in only a couple of samples from the northern part of the map area. Many of the rocks are cataclased to a greater

*11 Ca Mg Fe Si Al O
 .81 .69 .49 1.92 .08 6

or lesser extent. Where it is present, quartz occurs in grainy (sedimentary?) bands which suggest that these rocks are a mixture of volcanics with terrigenous products, rather than metabasalts.

Discussion:

The metamorphism of basalts is not fully understood, and in a study such as this, the petrogenetic work is made even less certain by the fact that the model for ocean-floor basalt is still relatively incomplete. In particular for the Slide Mountain Group, the question is one of sorting out the various processes which have generated the vast quantities of actinolite observed.

The abundance of zeolites (both real and suspected) would certainly suggest low metamorphic grade. AUMENTO *et al.* (1971) describe three levels of greenstone alteration. Ocean-water alteration affects the glass and the groundmass, but not the phenocrysts, and requires only very shallow burial, such as at the base of a flow. Zeolite facies alteration metamorphoses plagioclase into analcite, and the groundmass and glass into natrolite-mesolite-scolecite†stilbite†heulandite. Greenschist alteration metamorphoses plagioclase into albite, augite to actinolite, and olivine and glass to chlorite. These alterations are all accompanied by a major increase in water, but the iron oxidation ratio remains unchanged.

Of greater relevancy to the problem is the work of SEKI (1969) who describes three types of greenschist: pumpellyite-chlorite;

pumpellyite-actinolite-chlorite; and actinolite-chlorite facies. Of particular interest is the fact that epidote is stable from the middle of the pumpellyite-actinolite-chlorite facies upward. This assemblage of chlorite-epidote-actinolite \pm pumpellyite is very similar to what has been observed in the Clearwater Map Area.

Amphibolites may be formed over a wide range of compositions and greatly variable temperature and pressure conditions, making metamorphic interpretations difficult. In moderate grade metamorphism the stability of garnet is masked by amphibole whenever an excess of water is present (YODER and TILLEY, 1962). ERNST (1968) further describes the prograde metamorphism of amphibolites. The actinolite of the chlorite-biotite facies becomes a blue-green hornblende at the garnet facies. This in turn converts to a green hornblende at the staurolite-kyanite facies, and finally to a green or brown hornblende at the sillimanite facies. In an attempt to solve the retrograde/prograde problem in the MacKay River Map Area, we are left with the words of TILLEY and YODER in their 1962 classic:

Under equilibrium conditions it would not be possible to distinguish amphibolite and hornblende gabbro formed at the same pressure and temperature. Only the presence of non-equilibrium (relic) features may make it possible to determine whether or not such rocks came from the metamorphism of igneous rocks or were precipitated directly from liquid. In this sense the amphibolite problem is similar to the granite problem. p.469

PETROCHEMISTRY - MAJOR ELEMENTS:

Tholeiites:

The large majority of rocks within the Slide Mountain Group are tholeiites, and their chemical compositions are presented in Tables 1 and 2. For comparison, a number of averages are presented in Appendix 4. The basalt chemical screen has been well established as $\text{Al}_2\text{O}_3 > 10,5\%$; CaO 5-15%; and normative olivine $< 15\%$. There are a few rocks of this study that fall outside these (and other) criteria, but they are included since they form an integral part of the suite being studied.

When plotted on an AFM diagram (see Figure 9), only the low-Zr suite falls significantly away from the differentiation trend of average tholeiites. There is no tendency whatever to fall into the realm of alkali basalts.[§]

Silica is quite variable, but usually falls between 45-50%. Extreme values go about 3% beyond these limits, with lime and magnesia varying accordingly. Thus in some cases the strict basalt chemical screen is not met, but the overall chemical trends are still basaltic. Alumina presents much the same pattern and falls slightly lower than average. A curious point is the bimodal nature of alumina distribution, at 13,3% and 14,4%. Some rocks fall below the alumina limit, but present an overall tholeiitic aspect as regards alkalis, etc.

[text continues on page 44]

[§] The details of trace element chemistry and the resulting division into low- average- and high- Zr suites are explained in the next chapter.

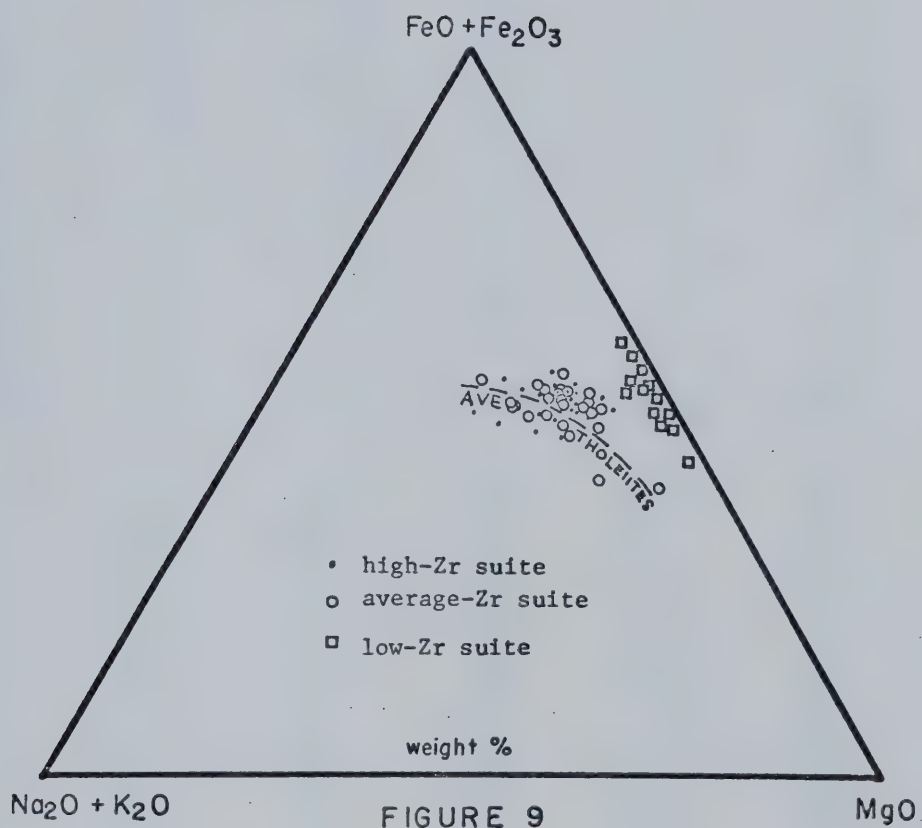


Figure 9: A F M Diagram

TABLE 1A: THOLEIITE / HIGH ZR SUITE

	[5550S]	[5551X]	[5551Y]	[5551Z]	[5552A]
SiO ₂	50,0	49,8	49,2	50,5	51,8
Al ₂ O ₃	14,8	12,4	15,7	13,1	14,4
Fe ₂ O ₃	3,14	3,33	3,14	3,10	3,13
FeO	8,49	9,00	8,47	8,38	8,46
MnO	,19	,23	,21	,20	,19
MgO	7,99	8,06	8,49	8,17	7,44
CaO	8,12	11,1	8,05	8,75	8,56
Na ₂ O	4,16	2,90	3,33	3,84	2,90
K ₂ O	,12	,08	,54	,20	,27
TiO ₂	1,79	1,79	1,68	1,94	1,66
P ₂ O ₅	,19	,18	,21	,18	,19
CO ₂	nil	,6	nil	,1	nd
H ₂ O #	1,0	,6	1,0	1,5	1,0
TOTAL	99,99	100,07	100,02	99,96	100,00

Li	9,9	nd	12,4	9,3	nd
S	800	1800	1300	6900	700
Sc	22	nd	21	26	nd
V	370	nd	330	310	nd
Cr	340	nd	360	340	nd
Co	60	nd	70	60	nd
Ni	102	84	98	86	nd
Cu	61	42	54	49	nd
Zn	102	105	107	96	97
Rb	1	2	12	3	3
Sr	210	240	270	190	190
Y	45	44	45	45	34
Zr	157	145	153	151	156
Nb	6	8	7	3	4
Mo	4	nd	4	8	nd
Ba	63	49	100	72	64
Pb	<10	nd	<10	<10	nd

* determined by titration

c determined by combustion

calculated by difference

Xo trace elements in ppm, non-significant places as (o)

nd not determined

TABLE 1B: THOLEIITE / HIGH ZR SUITE

	[5552B]	[5552Z]	[5553A]	[5553B]	[5553C]
SiO ₂	52,5	47,9	48,7	48,0	51,0
Al ₂ O ₃	14,6	13,1	14,9	13,1	14,4
Fe ₂ O ₃	2,99	3,34	3,37	3,29	3,19
FeO	8,07	9,03	9,11	8,88	8,62
MnO	,19	,21	,20	,21	,21
MgO	7,44	8,83	8,50	8,50	7,75
CaO	7,35	12,5	9,52	12,8	8,58
Na ₂ O	3,84	1,97	2,68	2,12	3,29
K ₂ O	,19	,08	,33	,05	,07
TiO ₂	1,68	1,74	1,72	1,72	1,63
P ₂ O ₅	,19	,22	,20	,20	,19
CO ₂	nd	nil	nil	nil	nil
H ₂ O #	1,0	1,1	,8	1,1	1,1
TOTAL	100,04	100,02	100,03	99,97	100,03
Li	nd	6,9	nd	nd	nd
S	400	1200	1500	2000	1100
Sc	nd	22	nd	nd	nd
V	nd	330	nd	nd	nd
Cr	nd	350	nd	nd	nd
Co	nd	60	nd	nd	nd
Ni	nd	103	114	116	nd
Cu	nd	59	62	59	nd
Zn	95	112	114	102	92
Rb	5	1	8	1	nil
Sr	160	150	230	160	180
Y	34	41	46	42	32
Zr	161	143	153	142	150
Nb	6	4	9	3	5
Mo	nd	5	nd	nd	nd
Ba	50	58	50	53	53
Pb	nd	nd	nd	nd	nd

* determined by titration

ç determined by combustion

calculated by difference

Xo trace elements in ppm, non-significant places as (o)

nd not determined

TABLE 1C: THOLEIITE / HIGH ZR SUITE

	[5553Y]	[5553Z]	[5554A]	[5554B]	[5555]
SiO ₂	49,8	48,6	50,8	52,0	49,8
Al ₂ O ₃	13,2	14,2	15,3	14,5	14,1
Fe ₂ O ₃	3,19	3,45	3,26	3,18	2,95
FeO	8,62	9,32	8,82	8,60	7,98
MnO	,21	,23	,19	,19	,20
MgO	8,13	8,69	7,24	6,95	7,19
CaO	11,3	8,92	8,18	8,40	10,7
Na ₂ O	2,49	3,12	3,01	3,05	3,66
K ₂ O	,11	,27	,14	,14	,65
TiO ₂	1,66	1,77	1,70	1,72	1,61
P ₂ O ₅	,19	,18	,19	,21	,17
CO ₂	,1	nil	nd	nd	nd
H ₂ O	1,1	1,2	1,2	1,1	1,0
TOTAL	100,00	99,95	100,03	100,04	100,04

Li	11,2	nd	nd	nd	nd
S	2000	1500	1900	1000	1500
Sc	21	nd	nd	nd	nd
V	330	nd	nd	nd	nd
Cr	280	nd	nd	nd	nd
Co	120	nd	nd	nd	nd
Ni	98	112	nd	nd	nd
Cu	63	55	nd	nd	nd
Zn	107	115	97	89	87
Rb	4	4	1	3	8
Sr	190	160	200	180	120
Y	41	46	35	33	31
Zr	144	151	158	160	149
Nb	6	6	2	5	4
Mo	6	nd	nd	nd	nd
Ba	57	100	55	62	160
Pb	10	nd	nd	nd	nd

* determined by titration

ç determined by combustion

calculated by difference

Xo trace elements in ppm, non-significant places as (o)

nd not determined

TABLE 1D: THOLEIITE / HIGH ZR SUITE

	[5556A]	[5556B]	[5556Y]	[5556Z]	[5558A]
SiO ₂	51,8	49,8	48,2	49,7	50,4
Al ₂ O ₃	14,4	14,7	14,5	14,8	14,4
Fe ₂ O ₃	3,09	3,25	2,90*	3,18	3,15
FeO	8,34	8,78	8,79*	8,59	8,50
MnO	,19	,20	,21	,19	,20
MgO	7,75	8,24	9,50	7,93	7,75
CaO	8,58	9,40	9,74	8,17	8,48
Na ₂ O	2,87	2,57	2,96	4,18	3,80
K ₂ O	,05	,07	,10	,10	,37
TiO ₂	1,66	1,74	1,74	1,83	1,72
P ₂ O ₅	,19	,21	,16	,20	,19
CO ₂	nd	nd	nil ‡	nil ‡	nd
H ₂ O #	1,1	1,1	1,2	1,1	1,0
TOTAL	100,02	100,06	100,00	99,97	99,96
Li	nd	nd	10,7	14,8	nd
S	1700	1300	2100	700	700
Sc	nd	nd	20	21	nd
V	nd	nd	340	380	nd
Cr	nd	nd	350	390	nd
Co	nd	nd	70	70	nd
Ni	nd	nd	86	104	nd
Cu	nd	nd	53	58	nd
Zn	100	96	99	105	96
Rb	nil	1	nil	3	10
Sr	120	130	110	210	150
Y	32	34	44	47	29
Zr	166	173	144	155	169
Nb	5	5	5	7	5
Mo	nd	nd	4	9	nd
Ba	46	50	61	54	190
Pb	nd	nd	10	40	nd

* determined by titration

‡ determined by combustion

calculated by difference

Xo trace elements in ppm, non-significant places as (o)

nd not determined

TABLE 1E: THOLEIITE / HIGH ZR SUITE

	[5604]	[5607]	[5613A]	[5614]	[5621]
SiO ₂	51,9	55,5	48,8	48,3	54,5
Al ₂ O ₃	14,3	14,0	13,3	13,2	14,7
Fe ₂ O ₃	3,46	2,59	3,45	3,41	2,74
FeO	9,34	6,99	9,31	9,19	7,40
MnO	,20	,14	,21	,22	,18
MgO	6,27	5,79	7,77	8,13	5,42
CaO	5,96	7,33	9,86	10,3	7,18
Na ₂ O	3,38	4,47	3,63	2,99	4,36
K ₂ O	1,16	,15	,08	,16	,60
TiO ₂	2,66	1,81	2,05	2,17	1,90
P ₂ O ₅	,22	,31	,21	,17	,21
CO ₂	,3	n11	,1	,34 c	n11
H ₂ O #	,6	,9	1,2	1,4	,8
TOTAL	100,05	99,98	99,97	99,98	99,99

Li	15,9	nd	9,4	7,8	nd
S	1300	1800	2700	6700	100
Sc	20	nd	22	18	nd
V	460	nd	390	330	nd
Cr	200	nd	280	270	nd
Co	70	nd	80	110	nd
Ni	39	13	82	80	26
Cu	40	790	51	56	9
Zn	129	90	132	115	68
Rb	27	4	2	3	19
Sr	140	40	180	190	210
Y	44	57	42	46	46
Zr	172	218	156	154	165
Nb	19	6	8	6	7
Mo	5	nd	3	4	nd
Ba	5900	300	90	150	1800
Pb	10	nd	10	<10	nd

* determined by titration

c determined by combustion

calculated by difference

Xo trace elements in ppm, non-significant places as (o)

nd not determined

TABLE 1F: THOLEIITE / HIGH ZR SUITE

	[5636]	[5636B]	[5636C]
SiO ₂	47,5	49,3	47,9
Al ₂ O ₃	14,4	14,8	14,2
Fe ₂ O ₃	3,83*	3,43	3,49
FeO	9,58*	9,27	9,42
MnO	,20	,20	,20
MgO	8,28	7,09	8,28
CaO	9,91	9,89	9,64
Na ₂ O	2,98	2,50	3,26
K ₂ O	,03	,27	,04
TiO ₂	1,87	1,93	2,12
P ₂ O ₅	,27	,23	,27
CO ₂	,01 c	,1	,1
H ₂ O #	1,2	1,0	1,1
TOTAL	100,06	100,01	100,02

Li	7,8	8,2	5,6
S	400	900	1000
Sc	21	25	19
V	370	400	330
Cr	280	230	250
Co	70	90	70
Ni	69	64	75
Cu	60	63	32
Zn	95	108	81
Rb	2	6	5
Sr	190	160	130
Y	43	46	44
Zr	158	161	156
Nb	7	5	6
Mo	5	4	3
Ba	200	590	230
Pb	<10	<10	<10

* determined by titration

c determined by combustion

calculated by difference

Xo trace elements in ppm, non-significant places as (o)

nd not determined

TABLE 2A: THOLEIITE / AVERAGE ZR SUITE

	[5550R]	[5550T]	[5550U]	[5550V]	[5550W]
SiO ₂	48,5	43,4	51,2	50,7	50,5
Al ₂ O ₃	13,7	13,0	13,1	13,6	13,9
Fe ₂ O ₃	3,31	3,65	2,88	2,87	2,52*
FeO	8,93	9,85	7,79	7,74	7,90*
MnO	,21	,24	,20	,19	,20
MgO	7,34	7,43	6,83	6,88	7,23
CaO	12,0	14,8	11,4	11,8	10,8
Na ₂ O	3,09	2,12	3,78	3,43	3,91
K ₂ O	,04	,04	,07	,13	,02
TiO ₂	1,66	2,12	3,78	3,43	3,91
P ₂ O ₅	,20	,20	,20	,18	,18
CO ₂	,04ç	n11	,1	n11	n11
H ₂ O #	1,0	3,1	,9	,8	1,0
TOTAL	100,02	99,95	100,03	100,02	99,99

Li	15,4	nd	11,1	nd	9,7
S	400	1500	1100	200	1900
Sc	22	nd	22	nd	27
V	380	nd	350	nd	370
Cr	270	nd	260	nd	350
Co	80	nd	90	nd	60
Ni	58	69	62	60	68
Cu	49	72	52	51	64
Zn	79	85	74	66	70
Rb	1	1	1	4	1
Sr	80	57	69	80	100
Y	36	40	34	35	41
Zr	109	128	110	115	128
Nb	6	5	6	7	4
Mo	6	nd	5	nd	6
Ba	60	66	66	75	56
Pb	10	nd	10	nd	<10

* determined by titration

ç determined by combustion

calculated by difference

Xo trace elements in ppm, non-significant places as (o)

nd not determined

TABLE 2B: THOLEIITE / AVERAGE ZR SUITE

	[5550X]	[5550Y]	[5550Z]	[5557]	[5557Z]
SiO ₂	51,9	45,0	49,1	48,6	50,4
Al ₂ O ₃	14,5	14,2	14,7	14,3	14,1
Fe ₂ O ₃	2,75	4,03	3,31	3,33	2,87
FeO	7,43	10,9	8,93	8,99	7,75
MnO	,15	,16	,17	,19	,19
MgO	5,60	8,38	7,64	8,53	8,57
CaO	10,3	11,6	9,51	9,77	9,51
Na ₂ O	4,33	2,30	3,68	3,11	3,50
K ₂ O	,09	,11	,08	,04	,14
TiO ₂	1,59	1,87	1,73	1,82	1,76
P ₂ O ₅	,17	,16	,17	,18	,17
CO ₂	,2	,3	nil	nil	,1
H ₂ O #	1,0	1,0	1,0	,6	,9
TOTAL	100,01	100,06	100,02	100,06	99,96

Li	nd	nd	15,5	nd	nd
S	3300	600	600	1600	1900
Sc	nd	nd	20	nd	nd
V	nd	nd	370	nd	nd
Cr	nd	nd	240	nd	nd
Co	nd	nd	90	nd	nd
Ni	44	56	61	64	84
Cu	49	73	56	61	60
Zn	67	112	143	105	99
Rb	2	1	3	nil	2
Sr	64	62	58	143	125
Y	37	37	39	40	37
Zr	118	120	125	130	124
Nb	7	4	6	4	6
Mo	nd	nd	9	nd	nd
Ba	53	84	63	45	53
Pb	nd	nd	< 10	nd	nd

* determined by titration

ç determined by combustion

calculated by difference

Xo trace elements in ppm, non-significant places as (o)

nd not determined

TABLE 2C: THOLEIITE / AVERAGE ZR SUITE

	[5558B]	[5558Z]†	[5602]	[5603]	[5606]
SiO ₂	51,3	42,7	52,5	49,6	48,3
Al ₂ O ₃	15,1	12,6	13,4	9,69	14,3
Fe ₂ O ₃	2,84	4,09	2,93	3,00	3,21
FeO	7,67	11,1	7,92	8,11	8,68
MnO	,18	,27	,18	,19	,21
MgO	7,43	12,1	6,16	7,07	8,40
CaO	7,87	12,0	11,4	19,1	9,37
Na ₂ O	4,79	1,08	2,69	,50	2,12
K ₂ O	nil	,56	,06	nil	2,26
TiO ₂	1,61	1,87	1,60	1,37	1,86
P ₂ O ₅	,17	,17	,14	,15	,17
CO ₂	nd	nil	nil	,006¢	,4
H ₂ O #	1,0	1,5	1,0	1,3	,7
TOTAL	99,96	100,04	99,98	100,09	99,98
Li	nd	13,1	11,4	5,5	14,9
S	2100	2400	1400	3100	1600
Sc	nd	27	17	23	25
V	nd	340	340	310	350
Cr	nd	420	210	450	360
Co	nd	70	70	70	90
Ni	nd	103	46	89	72
Cu	nd	51	86	57	88
Zn	93	111	95	84	100
Rb	nil	9	1	2	55
Sr	170	59	50	19	230
Y	29	43	34	27	32
Zr	129	138	113	82	119
Nb	2	3	4	2	13
Mo	nd	5	6	6	3
Ba	63	82	44	70	3400
Pb	nd	< 10	< 10	20	30

* determined by titration

¢ determined by combustion

calculated by difference

Xo trace elements in ppm, non-significant places as (o)

nd not determined

† non-tholeiite included because of Zr association

TABLE 2D: THOLEIITE / AVERAGE ZR SUITE

	[5608]	[5610]	[5610A]	[5611B]	[5611C]
SiO ₂	47,9	49,3	46,2	51,6	50,7
Al ₂ O ₃	14,5	15,8	16,6	14,2	14,8
Fe ₂ O ₃	2,26*	3,11	3,46	3,10	3,00
FeO	10,0 *	8,40	9,35	8,38	8,10
MnO	,22	,19	,21	,22	,16
MgO	8,33	10,5	12,1	7,65	8,36
CaO	10,8	6,09	5,66	7,01	6,28
Na ₂ O	2,90	3,67	3,21	4,11	4,30
K ₂ O	,14	,25	,20	,76	,53
TiO ₂	1,41	1,57	1,67	1,72	1,85
P ₂ O ₅	,21	,12	,13	,15	,14
CO ₂	,006¢	nil	nil	,1	,3
H ₂ O #	1,3	1,0	1,2	1,0	1,5
TOTAL	99,98	100,00	99,99	100,00	100,02

Li	14,6	42,1	nd	21,9	nd
S	2400	1100	2400	1600	8000
Sc	22	21	nd	22	nd
V	350	350	nd	330	nd
Cr	200	360	nd	300	nd
Co	80	70	nd	80	nd
Ni	72	94	99	81	73
Cu	64	56	39	50	36
Zn	115	108	127	111	116
Rb	4	7	4	10	9
Sr	260	260	250	190	160
Y	34	32	37	39	41
Zr	105	103	116	116	124
Nb	19	5	6	5	4
Mo	3	8	nd	4	nd
Ba	241	430	300	550	430
Pb	<10	<10	nd	<10	nd

* determined by titration

¢ determined by combustion

calculated by difference

Xo trace elements in ppm, non-significant places as (o)

nd not determined

TABLE 2E: THOLEIITE / AVERAGE ZR SUITE

	[5615]	[5616]†	[5617]	[5618]	[5619]
SiO ₂	47,6	44,6	52,5	48,0	49,4
Al ₂ O ₃	15,2	12,3	13,2	14,2	14,6
Fe ₂ O ₃	3,78*	3,55	2,90	3,16	3,23
FeO	7,87*	9,59	7,83	8,55	8,73
MnO	,18	,21	,17	,20	,19
MgO	10,7	10,1	7,41	10,3	8,27
CaO	8,89	15,6	8,82	9,93	8,44
Na ₂ O	2,71	,61	3,64	2,58	3,44
K ₂ O	,55	,52	,50	,39	,66
TiO ₂	1,46	1,62	1,80	1,55	1,71
P ₂ O ₅	,15	,16	,17	,23	,16
CO ₂	,26ç	,1	n11	n11	n11
H ₂ O #	,6	1,1	1,1	,9	1,2
TOTAL	99,95	100,06	100,04	99,99	100,03
Li	8,3	8,8	6,5	12,8	6,2
S	500	1000	1400	600	1500
Sc	21	23	22	23	23
V	320	330	360	370	330
Cr	370	270	330	530	350
Co	70	70	80	80	80
Ni	114	87	95	116	85
Cu	35	58	59	50	60
Zn	97	94	94	100	93
Rb	9	11	9	10	2
Sr	210	40	170	290	90
Y	31	30	37	37	37
Zr	105	101	134	124	126
Nb	4	6	4	3	8
Mo	3	5	2	5	3
Ba	172	100	79	77	66
Pb	<10	<10	<10	10	<10

* determined by titration

ç determined by combustion

calculated by difference

Xo trace elements in ppm, non-significant places as (o)

nd not determined

† non-tholeiite included because of Zr association

TABLE 2F: THOLEIITE / AVERAGE ZR SUITE

	[5619A]	[5620]	[5630]	[5630B]
SiO ₂	51,4	48,5	47,4	50,1
Al ₂ O ₃	14,6	12,6	13,4	14,2
Fe ₂ O ₃	2,78	3,34	3,56*	3,03
FeO	7,51	9,02	9,57*	9,58
MnO	,15	,18	,24	,18
MgO	8,09	9,07	10,8	9,32
CaO	8,16	12,0	10,2	9,03
Na ₂ O	4,42	2,40	2,15	3,19
K ₂ O	,07	,06	,16	,10
TiO ₂	1,71	1,62	1,22	1,40
P ₂ O ₅	,17	,21	,21	,20
CO ₂	n11	,6	,13¢	n11
H ₂ O #	,9	,4	1,0	n11
TOTAL	99,96	100,00	100,04	100,03

Li	6,9	11,0	21,0	19,9
S	1200	100	200	2200
Sc	17	22	21	21
V	320	330	340	330
Cr	250	310	520	460
Co	80	80	70	70
Ni	69	70	97	99
Cu	55	59	27	10
Zn	115	97	143	97
Rb	16	1	6	2
Sr	190	130	180	160
Y	36	33	36	38
Zr	124	105	123	135
Nb	6	3	5	6
Mo	4	3	5	9
Ba	99	109	320	258
Pb	<10	10	10	<10

* determined by titration

¢ determined by combustion

calculated by difference

Xo trace elements in ppm, non-significant places as (o)

nd not determined

Potash is perhaps the most frequently discussed variable in tholeiite chemistry, and it can be an effective discriminator of tholeiite origin. Oceanic tholeiites are reported (HART, *et al.*, 1970) to contain about 0,14% K_2O compared to 0,40% for island arc tholeiites and much higher values for continental tholeiites. Potash in the tholeiites of this study is bimodal at 0,13% and around 0,30%. While the former figure is very close to the average for oceanic tholeiites, the latter mode approaches the value for island arc tholeiites. This precludes a definitive interpretation of the entire suite as oceanic tholeiite on the basis of potash alone.

In dealing with rocks that have been metamorphosed it is a questionable practice to rely on one element, particularly an alkali. PEARCE *et al.* (1975) have developed the use of the $TiO_2 - K_2O - P_2O_5$ diagram (see Figure 10) as a way of distinguishing continental basalts from oceanic basalts. For these elements metamorphic alteration parallels the weathering trend in that the rock loses $Ti > K > P$. If weathering or metamorphism has been severe, the rocks tend to move towards the P_2O_5 apex, or away from the oceanic basalt field. Thus if a metamorphosed basalt falls within the oceanic basalt field, it is very likely of oceanic origin.

Given that the Slide Mountain Group has been metamorphosed, the tendency of virtually all rocks to plot within the oceanic field is most surprising. This can be taken as a strong confirmation that the vast majority of the tholeiites are indeed oceanic tholeiites. The potash levels further support the contention

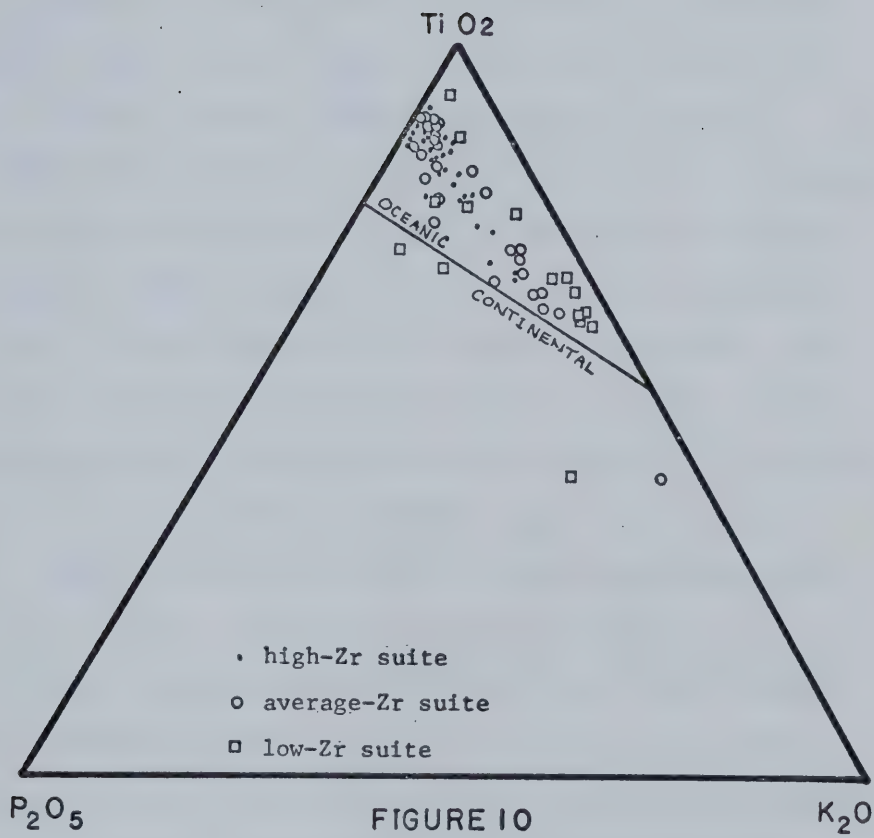
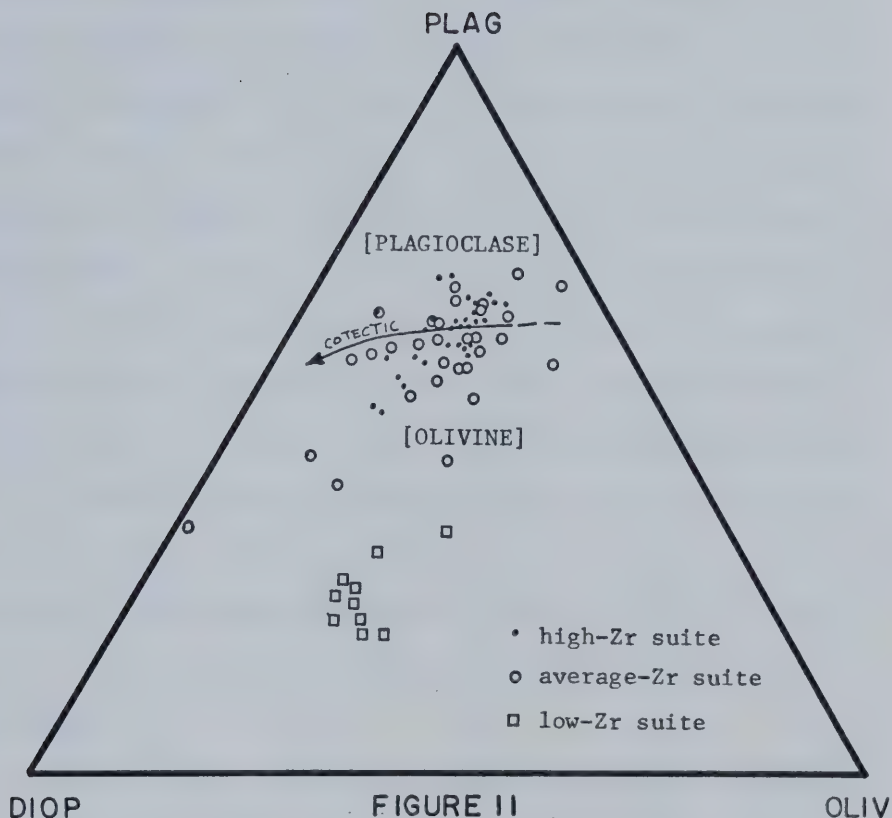


Figure 10: TiO_2 - K_2O - P_2O_5 Diagram

that the suite as a whole is associated with the generation of ocean-floor rather than island arcs.

When the whole-rock chemistry is viewed as a normative mineralogical assemblage (see Appendix 2), the plagioclase-diopside-olivine-quartz tetrahedron is accurate as a first approximation, and all the rocks of this study can be plotted on a plagioclase-diopside-olivine ternary diagram, since most have less than ten percent normative quartz. These are presented in Figure 11.

SHIDO *et al.* (1971) have discussed the order of crystallisation observed in tholeiites, and find that tholeiites may be divided into those in which olivine is the first mineral to crystallise and those in which plagioclase is the first to crystallise. If tholeiites are plotted on a ternary diagram of normative olivine-diopside-plagioclase, the rocks may divide cleanly into two groups, separated by a line which corresponds to the cotectic at 16,5% Al_2O_3 . While the rocks of this study contain significantly less alumina than 16,5%, it is notable that the high-alumina group (mode 14,4%) fall on the plagioclase-first side of the cotectic and the low-alumina group fall on the olivine-first side. This division seems to be more than coincidental, and though metamorphism has made it impossible to determine from thin sections whether olivine or plagioclase was the first mineral to crystallise in the rocks of this study, it would appear that the location of the cotectic is fairly tolerant to alumina variation. The cotectic should, however, move with changing pressure, and the fact that it



NB: The points from the Slide Mountain Group are plotted on the basis of their *normative* mineralogy. The minerals in brackets [] show the fields where those minerals are *observed* by SHIDO *et al.* (1971) to be the first to crystallise in rocks of a normative composition falling in that field.

Figure 11: Normative Plagioclase-Olivine-Diopside Diagram

does not suggest that the range of pressures at which tholeiites crystallise is rather limited.

The presence of a number of rocks of normative compositions which fall into SHIDO *et al.*'s field suggests a couple of possibilities, bearing in mind KUNO's (1967) discussion of the lack of olivine in tholeiites. The first is that with lower alumina the cotectic would move away from the plagioclase apex, or that with alteration the normative mineralogy is shifted and the cotectic remains fixed. If this is so, then the bimodal alumina distribution becomes meaningless. The second possibility is raised by MIYASHIRO *et al.* (1970) who contend that in abyssal tholeiites olivine continues to crystallise through the groundmass stage instead of reacting with Ca-poor pyroxene as is the case with continental tholeiites. This is certainly compatible with the data, and there is thus a good probability that the tholeiites of this study crystallised near the olivine-plagioclase cotectic.

Komatiites:

Although clearly of oceanic origin on the basis of Figure 10, the low-Zr suite of this study presents a number of chemical problems. Most obvious is the alumina-poor nature of the rocks (see Table 3), averaging about 7,5% but often much lower. This is accompanied by a substantial reduction in soda to under 0,5% and occasionally to nil. Conversely, iron and magnesia are substantially enriched.

Elemental migration during early (submarine) alteration can be conclusively ruled out. Research on the alteration of submarine

TABLE 3A: KOMATIITE / LOW ZR SUITE

	[5720] [@]	[5720A] [@]	[5721] [@]	[5721A] ⁺	[5721B] ⁺
SiO ₂	45,4	46,3	45,8	45,6	47,4
Al ₂ O ₃	5,83	6,00	5,94	7,35	7,45
Fe ₂ O ₃	4,74	4,30	5,25*	4,53*	3,53
FeO	12,8	11,6	11,8 *	10,5 *	9,53
MnO	,21	,21	,22	,22	,23
MgO	14,5	15,5	14,8	15,1	14,8
CaO	12,6	12,7	12,9	15,1	14,8
Na ₂ O	,59	,23	,57	,44	,03
K ₂ O	,51	,46	,25	,15	,13
TiO ₂	1,27	1,21	1,06	,85	,73
P ₂ O ₅	,05	,07	,05	,19	,25
CO ₂	nil	nil	,09¢	,46¢	nd
H ₂ O #	1,5	1,0	1,2	,6	1,4
TOTAL	100,00	99,98	99,97	99,99	100,03
Li	15,0	nd	11,9	16,4	nd
S	1300	600	600	nil	300
Sc	45	nd	52	47	nd
V	570	nd	510	440	nd
Cr	710	200	390	330	400
Co	90	nd	110	70	nd
Ni	116	124	113	52	nd
Cu	71	102	219	54	31
Zn	96	82	96	98	84
Rb	13	11	6	4	11
Sr	200	230	400	450	380
Y	13	12	13	15	15
Zr	16	16	21	22	18
Nb	1	nil	1	1	1
Mo	3	nd	4	5	nd
Ba	150	120	120	100	64
Pb	10	nd	<10	<10	nd

* determined by titration

¢ determined by combustion

calculated by difference

Xo trace elements in ppm, non-significant places as (o)

nd not determined

@ passes chemical screen of VILJOEN and VILJOEN (1969a)

+ passes chemical screen of BROOKS and HART (1974)

TABLE 3B: KOMATIITE / LOW ZR SUITE

	[5722]@	[5722B]@	[5722C]@	[5723]@	[5724]@
SiO ₂	41,6	43,8	44,6	41,9	43,9
Al ₂ O ₃	6,84	6,62	7,89	5,04	5,55
Fe ₂ O ₃	4,94	4,50	4,17	4,80	4,49
FeO	13,3	12,1	11,3	13,0	12,1
MnO	,22	,22	,22	,16	,20
MgO	14,4	14,2	14,4	15,6	16,7
CaO	15,2	15,3	14,7	16,4	13,9
Na ₂ O	,44	,08	,10	,38	,53
K ₂ O	,13	,12	,16	,04	,09
TiO ₂	1,21	1,18	1,11	1,27	1,11
P ₂ O ₅	,19	,35	,12	,06	,07
CO ₂	nil	nd	nd	,003¢	nil
H ₂ O #	1,5	1,5	,6	1,5	1,4
TOTAL	99,97	99,97	100,07	100,05	100,04

Li	8,3	nd	nd	9,4	14,8
S	nil	600	200	nil	nil
Sc	60	nd	nd	56	63
V	620	nd	nd	590	570
Cr	240	200	200	470	490
Co	150	nd	nd	80	110
Ni	67	51	48	87	84
Cu	41	50	8900	11	13
Zn	127	124	810	87	142
Rb	6	5	3	1	1
Sr	300	270	480	70	100
Y	14	16	14	10	12
Zr	21	17	15	14	17
Nb	3	2	2	3	nil
Mo	4	nd	nd	2	4
Ba	89	160	49	55	83
Pb	410	nd	nd	10	410

* determined by titration

¢ determined by combustion

calculated by difference

Xo trace elements in ppm, non-significant places as (o)

nd not determined

@ passes chemical screen of VILJOEN and VILJOEN (1969a)

+ passes chemical screen of BROOKS and HART (1974)

TABLE 3C: KOMATIITE / LOW ZR SUITE

	[5725] ⁺	[5725A] ⁺	[5726] [@]	[5726A] ⁺	[5727]
SiO ₂	38,1	41,0	44,7	46,6	50,4
Al ₂ O ₃	10,9	11,8	7,97	9,57	8,31
Fe ₂ O ₃	5,81	5,14	4,00	3,38	3,02
FeO	15,7	13,9	10,8	9,13	8,15
MnO	,28	,28	,23	,22	,23
MgO	15,2	15,7	14,1	14,3	15,5
CaO	10,6	9,23	15,2	14,6	10,3
Na ₂ O	,38	nil	,44	,04	1,61
K ₂ O	,07	,08	,19	,12	,61
TiO ₂	,87	,89	,93	,72	,64
P ₂ O ₅	,40	,41	,31	,22	,21
CO ₂	,3	nd	nil	nd	,1
H ₂ O #	1,4	1,6	1,1	1,1	,9
TOTAL	100,01	100,03	99,97	100,00	99,98
Li	6,2	nd	12,6	nd	9,4
S	nil	200	nil	100	200
Sc	32	nd	48	nd	42
V	600	nd	490	nd	330
Cr	510	200	190	400	590
Co	110	nd	110	nd	80
Ni	66	71	63	47	94
Cu	16	61	77	8700	67
Zn	151	149	91	920	101
Rb	4	nil	5	3	11
Sr	510	460	770	660	460
Y	10	10	15	15	13
Zr	9	nil	20	7	20
Nb	1	nil	1	nil	2
Mo	3	nd	3	nd	3
Ba	45	19	109	59	161
Pb	10	nd	10	nd	< 10

* determined by titration

ç determined by combustion

calculated by difference

Xo trace elements in ppm, non-significant places as (o)

nd not determined

@ passes chemical screen of VILJOEN and VILJOEN (1969a)

+ passes chemical screen of BROOKS and HART (1974)

basalt (MIYASHIRO *et al.*, 1969; HART, 1970) shows a trend opposite to that found in this study. Typically altered submarine basalts are strongly depleted in magnesia and lime with relation to alumina and are often enriched in soda. Since basic rocks undergo no chemical changes during metamorphism up to the upper amphibolite facies (SIGHINOLFI, 1971) the whole-rock chemistry of the low-Zr suite is almost certainly primary, or very nearly so.

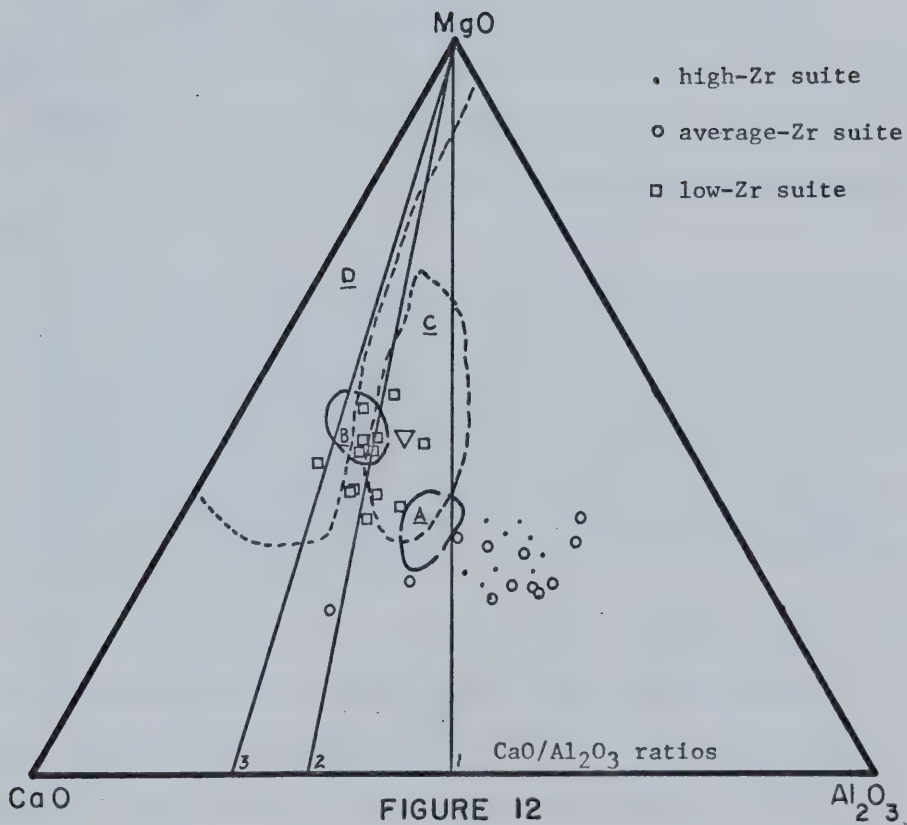
Komatiites were first described as a separate class of rocks by VILJOEN and VILJOEN (1969*a*, 1969*b*, 1970) and it was suggested that komatiites were a feature peculiar to Precambrian terranes, probably evolved from the mantle before it had begun to differentiate. This theory was expanded somewhat by BROOKS and HART (1972) who reported an Archaean komatiite from the Canadian Shield and postulated an island arc genesis for it. The notion that komatiite was a peculiarity of the Precambrian was destroyed by the confirmation that a number of lower Cambrian rocks in Newfoundland were, indeed, komatiites (GALE, 1973).

The Viljoens divided the class of komatiites into two major groups: basaltic komatiites and peridotitic komatiites, and it is with the first of these that this study is concerned. In fact, no Phanerozoic peridotitic komatiites have been reported. The basaltic komatiites were further divided into the types present at Badplaas and at Barberton and into a high-alumina type. These have since become the standards against which other komatiites are compared, though their usefulness is diminishing because they were based on a highly localised examination of rocks, with little attention paid to similar rocks elsewhere.

When BROOKS and HART (1972) plotted their Canadian komatiite on a $\text{CaO-MgO-Al}_2\text{O}_3$ diagram (see Figure 12) it plotted more or less between the Barberton and Badplaas fields, the first suggestion that komatiites are a much more varied class of rocks than was first believed. Though the low-Zr suite of the Slide Mountain Group, all from the MacKay River Map Area, plots in the general vicinity of the Badplaas komatiites, it moves away from that field in several directions.

BROOKS and HART (1974) modified the interpretation of the $\text{CaO-MgO-Al}_2\text{O}_3$ diagram considerably after a computer search of rocks of komatiitic composition. They added two large fields which project onto the diagram but represent non-komatiites. Many of the rocks classified as picrites, oceanites, and ankaramites pass the Viljoens' chemical screen ($\text{MgO} > 9\%$; $\text{CaO/Al}_2\text{O}_3 > 1$; and $\text{K}_2\text{O} < 0.9\%$) but all have TiO_2 values (average 2.2%) higher than those reported by the Viljoens, and are generally higher in K_2O . This picrite-oceanite-ankaramite field is shown on Figure 12, as is the peridotite-pyroxenite field also proposed by BROOKS and HART (1974).

Of particular interest, too, is that from the handful of tholeiites plotted for comparison, a few approach the Barberton field very closely. Thus while tholeiites as a class plot near the Barberton field (nearer to it than do the Badplaas komatiites) there is some cause to believe that a continuum relationship might exist for the rocks of this study. This is reinforced by the existence of two 'tholeiites' ([5558Z] and [5616]) in the average



- (A) Barberton Komatiites (VILJOEN and VILJOEN, 1969a)
- (B) Badplaas Komatiites (*ibid.*)
- (C) Picrite-Oceanite-Ankaramite field of BROOKS and HART (1974)
- (D) Peridotite-Pyroxenite field (*ibid.*)
- ▽ Canadian Komatiite (BROOKS and HART, 1972)

Figure 12: MgO - Al₂O₃ - CaO Diagram

Zr suite with abnormally low silica and alumina.

CAWTHORN and STRONG (1974) have raised a similar problem, finding that even the chemical screen of BROOKS and HART (1974) ($\text{MgO} < 9\%$; $\text{CaO}/\text{Al}_2\text{O}_3 < 1$; $\text{K}_2\text{O} < 0,9\%$ {most $< 0,5\%$ }; and $\text{TiO}_2 < 0,9\%$) was not effective in separating komatiites from other rocks. Using the screen of BROOKS and HART (1974), better than half of the 'komatiites' of this study are eliminated on the basis of high TiO_2 .

CAWTHORN and STRONG (1974) move from these very real difficulties with komatiitic bulk chemistry to make the following statement:

The alleged chemical characteristics of komatiites are not unique. We therefore suggest that komatiite is not a distinctive isolated new class of basic and ultrabasic rocks, but a more extreme composition in a spectrum of rocks with chemical characteristics imposed by shallow depth and a high degree of partial melting. ... The only reported Phanerozoic komatiites so far identified occur in close association with oceanic tholeiites and ophiolites. These isolated occurrences may be explained by slightly shallower depth of melting than usual for oceanic tholeiites because of locally very high geothermal gradients on mid-ocean ridges.

While this study does not support such an extreme position as this, the statement does effectively outline the problem of trying to develop, both chemically and tectonically, simplified models for natural systems. There is good evidence that the komatiites of this study were intruded as pyroxenites, and this *might* correspond to a model taken from the Vourinos Ophiolitic Complex (MOORES, 1969) in which the very margins of the complex contain pyroxenites in direct involvement with tholeiitic basalt and volcanics. However, in the Vourinos rocks the alumina is but 2% of the total.

BROOKS and HART (1974) proceed further to insist on a textural discrimination for komatiites, in that the rocks must have been shown to have been liquid. Thus [5727] which is clearly schistose, though passing the komatiite screen (TiO_2), is clearly not an intrusive rock. This lends further support to the authors' contention that K_2O should be under 0,50% in komatiites, since K_2O for [5727] is somewhat greater than that value.

A number of komatiitic analyses are presented for comparison in Appendix 5, and while there is much in common amongst them, they are, nonetheless, a highly varied class of rocks. That komatiites are a different class of rocks can not be convincingly challenged, but neither can accurate definitions and chemical screens be established until more data are available.

PETROCHEMISTRY - TRACE ELEMENTS:

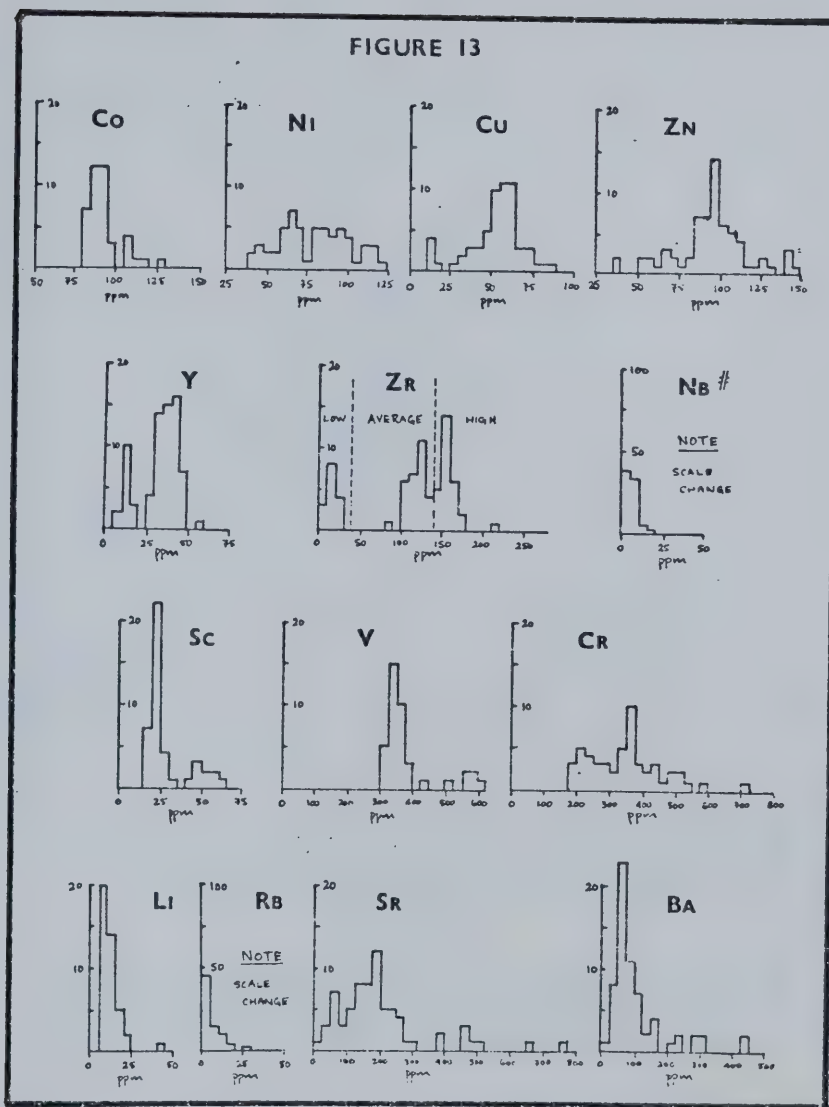
Introduction:

As the level of geochemical interpretation becomes increasingly more complex, trace elements are becoming more important as interpretive tools.

One of the most useful methods of presenting trace element data is still the histogram (see Figure 13), though its usefulness in interpretation is limited. While the elements will be discussed in their turn, please note that the trimodal distribution of Zr has become the division upon which all discussions of both major and trace element chemistry have been based.

Yttrium and Niobium:

With Zr and Ti, Y and Nb are two trace elements which change very little during alteration. Changes in original abundances are not greater than ten percent (CANN, 1970). Yttrium is most abundant in apatite, but also substitutes for ferrous iron in ilmenite and magnetite (PRINZ, 1967). It is present in limited amounts in pyroxenes. Maximum Y values in basalts are 100 ppm (THOMPSON *et al.*, 1972), and the average for rocks of this study is 30 - 50 ppm (see Figure 13). Some Y is present even in very primitive rocks (see Figure 14) if the Thornton-Tuttle Differentiation Index is taken as being a reasonably accurate description of the degree of differentiation of a rock.



the horizontal scale here hides somewhat the similarity to Y and Zr. The main mode is at 6 ppm, with a minor mode at 1-2 ppm (see Figure 16)

Figure 13: Trace Element Histograms

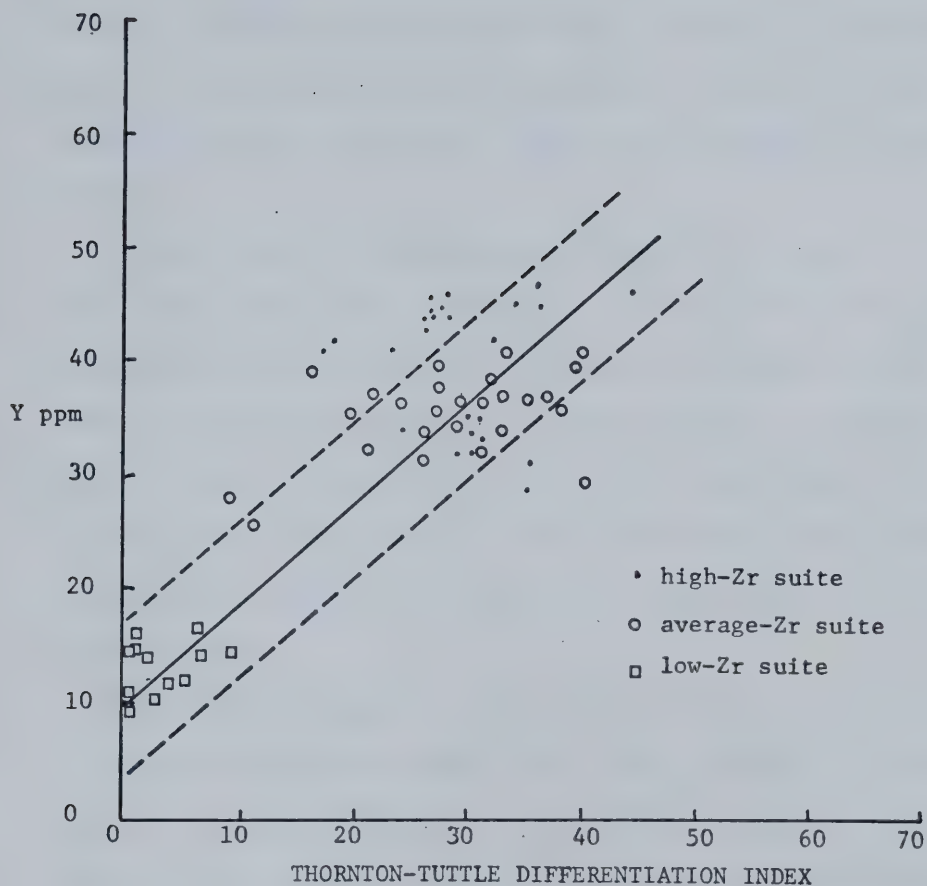


FIGURE 14

Note: In this and all similar graphs following, the pair of dashed lines has been added to indicate that both the location and the slope of the solid line may vary somewhat from that shown.

Figure 14: Y vs Thornton-Tuttle Differentiation Index

Even with rocks of differentiation index 0, 10 ppm Y is present, and this seems to be the lower limit for crustal rocks. Thus Y can be expected not only to be present in any basic rocks studied, but also to be non-mobile during alteration and metamorphism. It is a very useful element indeed, and its use in conjunction with CaO has been well developed by LAMBERT and HOLLAND (1974).

Figure 15 shows a marked division between the komatiites (the low-Zr suite) and the tholeiites. The komatiites show clearly a predominating orthopyroxene-clinopyroxene fractionation, with olivine as a minor component, since orthopyroxenes tend to be a bit too rich in Y to explain the plot fully. From Figure 15 it is also possible to postulate olivine-clinopyroxene fractionation, but this is not supported by other trace element data, as will be explained later.

The tholeiites appear to be very close to the average value for oceanic tholeiites (LAMBERT and HOLLAND, 1974) but are slightly lower in Y. Although they are scattered when compared to the komatiites, the tholeiite points fall between the pyrope and the clinopyroxene fields. This is compatible with a model of fractionation of a garnet peridotite, which was one of the possibilities considered by SCHILLING (1971) but not pursued due to the lack of reliable rare earth element partition coefficient data for garnet.

The main limit on the validity of a trace element model is that there are three different effects in operation: a source

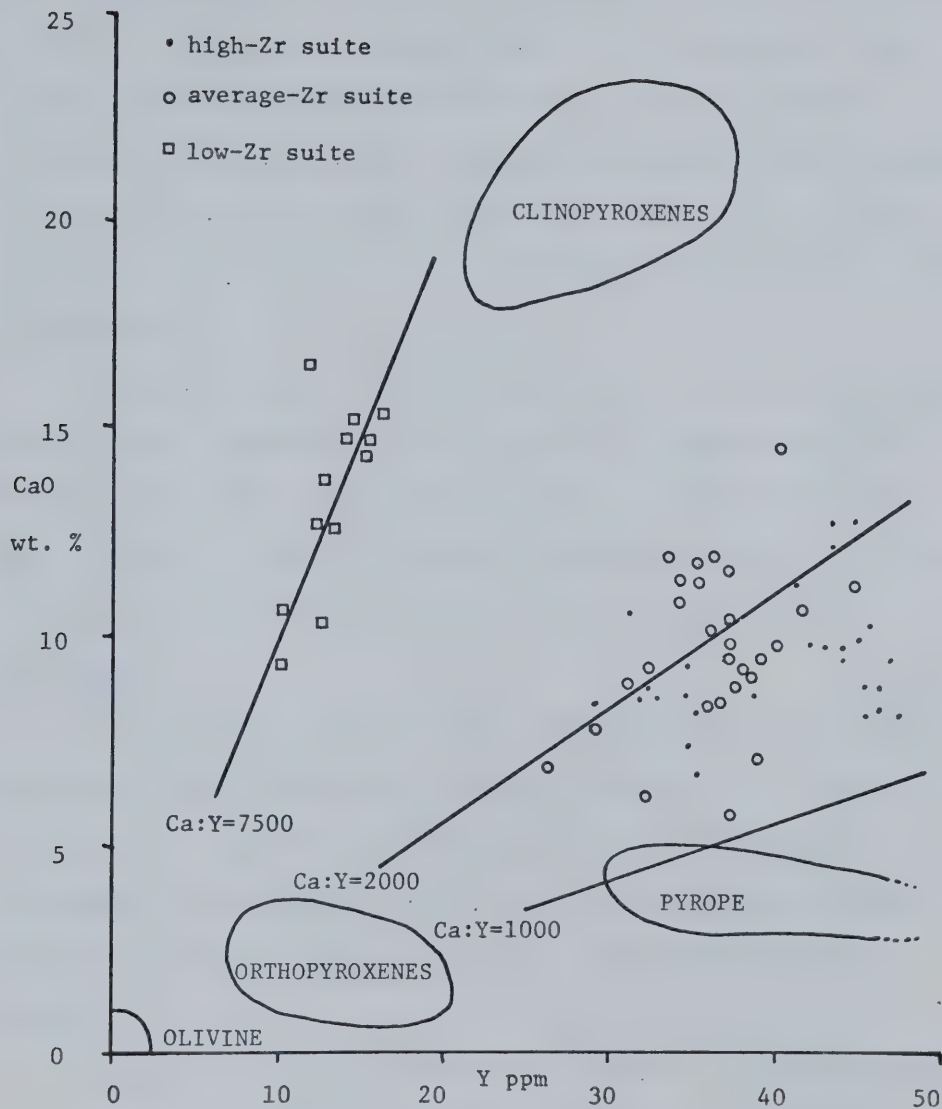


FIGURE 15

Figure 15: CaO vs Y

effect, a mineral effect (are they Y-acceptors or Y-rejectors?), and a mixing effect. The last can be easily eliminated since the Y values for this study correspond well with the average 39 ppm of the Juan de Fuca Ridge and the 29 ± 7 ppm Y for all oceanic tholeiites (SCHILLING, 1971). The first is reasonably well covered in Figure 14, but the second, although the model is met by Figure 15, would allow equally for the involvement of plagioclase and some other minerals.

Niobium is a very minor component of the rocks (see Figure 13) and is either dependent on Y (see Figure 16) or codependent with Y on another element. The main point of note is that the Y-Nb plot is nearly identical in aspect to those of the Deep Sea Drilling Project rocks, another confirmation of oceanic character.

Zirconium:

Concentrated in the pyroxenes of basaltic rocks, Zr does not exceed 550 ppm (THOMPSON *et al.* 1972). Its distribution in the rocks of this study is trimodal (see Figure 13), with peaks at 10-20 ppm; 120-130 ppm; and 150-160 ppm. These have been designated as the low-Zr suite, the average-Zr suite, and the high-Zr suite.

Zirconium is highly dependent on the level of differentiation of the rock (see Figure 17), falling to nil at differentiation index 0. This may be the result of dependency on Na (see Figure 18) or on Ti (see Figure 19) since both are present in pyroxenes, or more plausible, both Ti and Zr may be codependent on Na. Additional elements may control Zr, but this has not been evident.

Figure 16: Nb vs Y

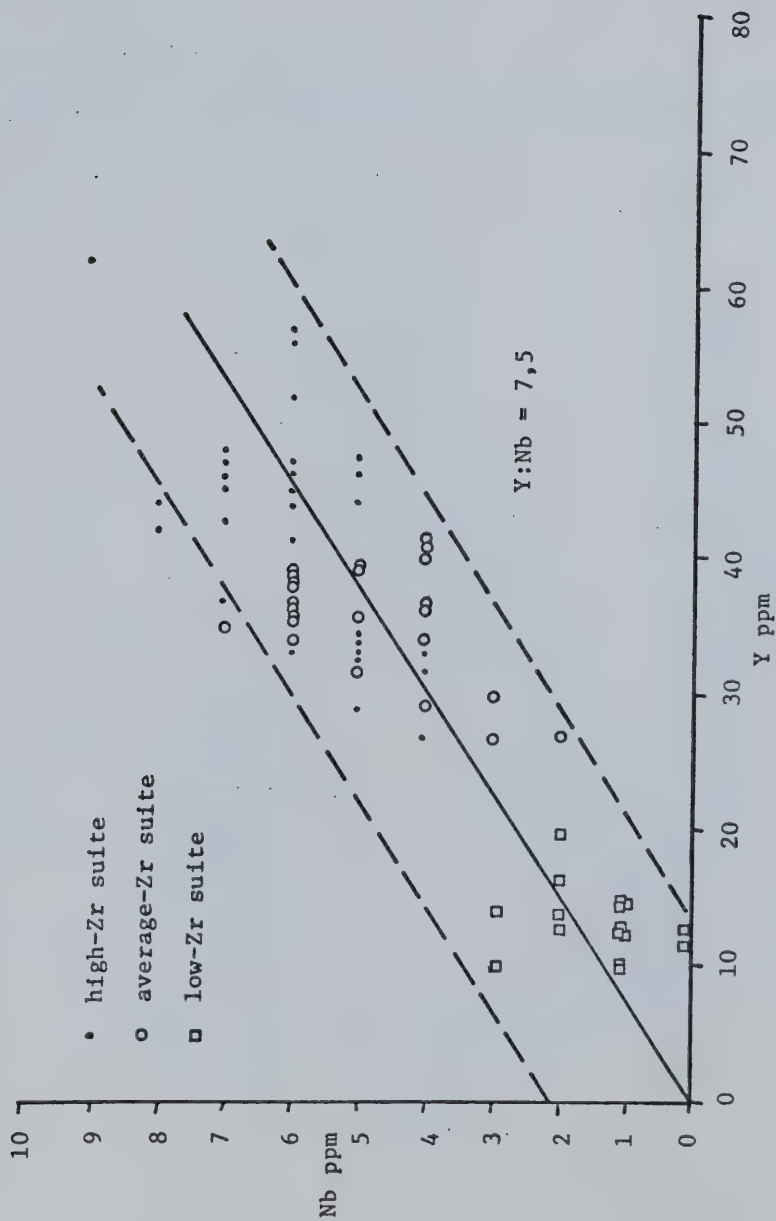


FIGURE 16

Figure 17: Zr vs Thornton-Tuttle Differentiation Index

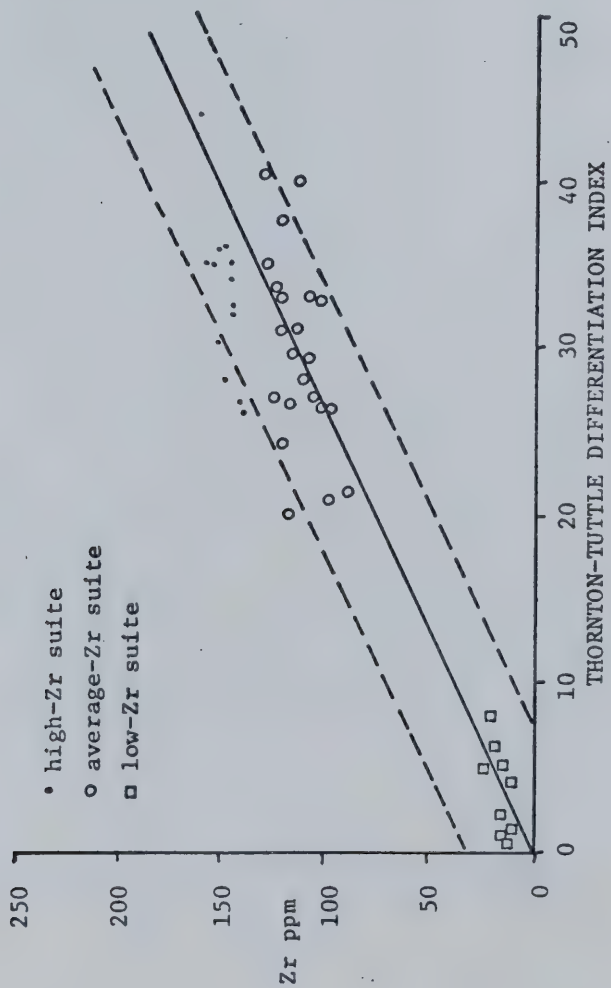


FIGURE 17

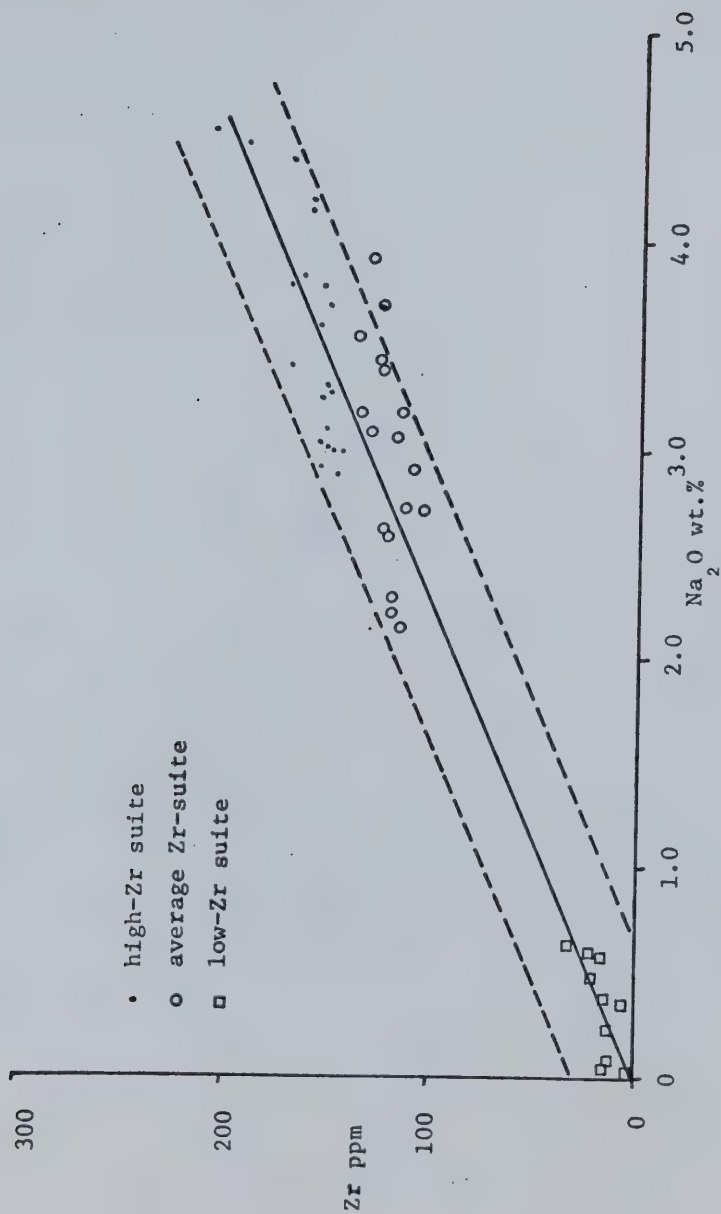
Figure 18: Zr vs Na_2O 

FIGURE 18

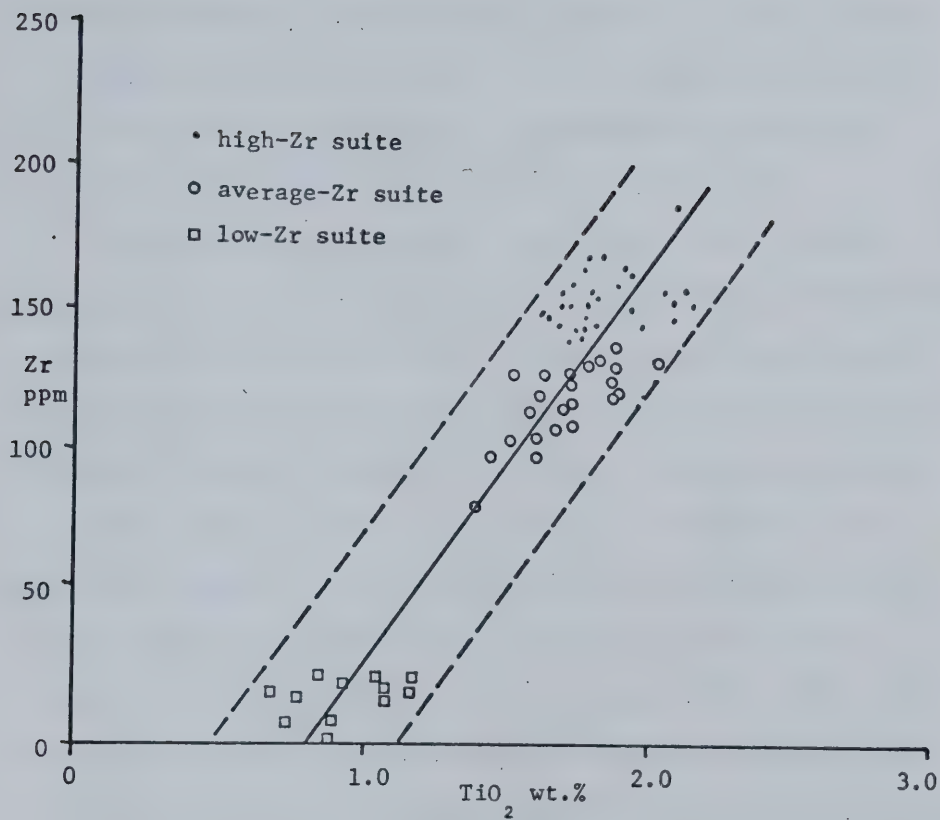


FIGURE 19

Figure 19: Zr vs TiO_2

In most rocks, 60-90% of Ti is present in the oxide phase, which would support the contention of codependency of Ti and Zr on Na. In highly magnesian rocks, however, the Ti tends to enter the silicate phase rather than the oxides (AL'MUKHADEMOM, 1967), but as Fe increases, Ti again tends to enter the oxides. Since the high-Mg rocks of this study also tend towards high-Fe, and have very low Zr (in the case of the komatiites), Ti may be eliminated as a controlling factor in Zr distribution.

The use of Zr in connection with Ti and Y as a means of characterising a basalt was first set out by PEARCE and CANN (1971) and applied by BICKLE and NISBET (1972) to the determination of the origin of some alpine mafic rocks. The method was further refined by PEARCE and CANN (1973) when the Y component was trebled in order to move the plot to the centre of the diagram. As shown by Figure 20, the average- and high-Zr suites (the tholeiites) form a tight grouping within the field of the oceanic tholeiites. This supports the TiO_2 - P_2O_5 - K_2O results (Figure 10) very well, with the exception that the komatiites, though oceanic in origin, do not plot within the field of the oceanic tholeiites.

It is not yet known where other komatiites will plot on the diagram, for few have been analysed for Zr, and even fewer for Y. Given the fairly scattered nature of the komatiite points compared to the tholeiite points, even for this one group of rocks, a separate komatiite field would seem unlikely because their composition is too extreme.

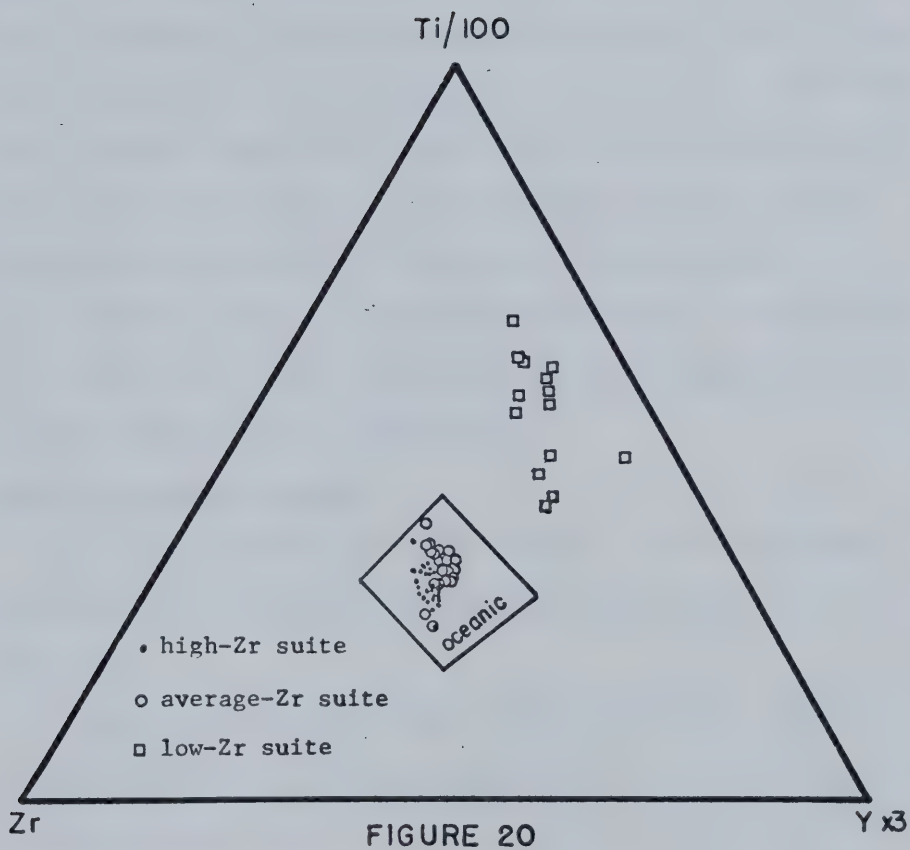


Figure 20: $\text{Ti}/100$ - $\text{Y} \times 3$ - Zr Diagram

Lithium:

Occupying some Fe and Mg sites, Li does not exceed 40 ppm in basaltic rocks (THOMPSON *et al.* 1972) and averages 10-15 ppm in the rocks of this study (see Figure 13). However, no dependency of Li on Mg exists in these rocks, as shown by Figure 21, which is unusual. It appears that there was either little olivine involvement or that most of the Mg sites were occupied early when the Li concentrations were too low for it to be accepted into the structure of pyroxene. It is probably found, instead, in the A-sites of the amphiboles. That the Slide Mountain Group is poorly differentiated has already been established, but the failure of the Li:Mg ratio to rise with differentiation suggests a narrow range of differentiation (PRINZ, 1967).

Rubidium-Strontium-Barium:

Rubidium is found only in the feldspars, and in the rocks of this study it is present at less than 5 ppm in most cases (see Figure 13).

Strontium is much more widely distributed and is usually found in clinopyroxenes, apatite, and plagioclases (especially An_{10-70}). Clinopyroxene has far less Sr than coexisting plagioclase (PRINZ, 1967) so most of the Sr in the tholeiites is in the plagioclases, and in the komatiites, in the pyroxenes. The average value of 100-200 ppm for the rocks of this study is well under the maximum value of 2200 ppm reported by THOMPSON *et al.* (1972). It has been used by PEARCE and CANN (1973) with Ti and Zr as another trace element discriminator for ocean-floor basalts. It has the

Figure 21: Li vs MgO

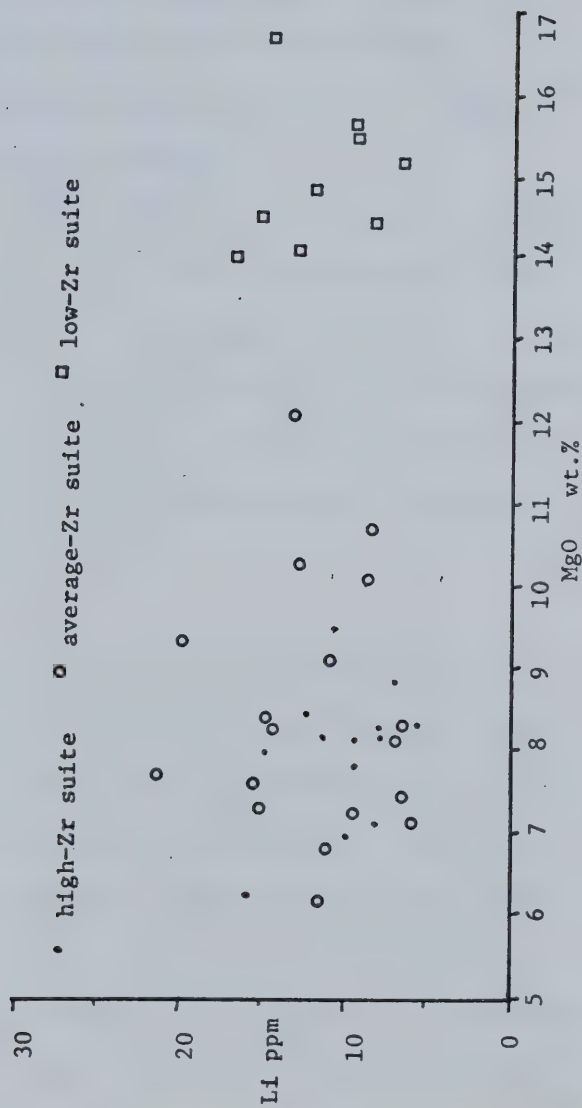


FIGURE 21

unfortunate limitation that it is reliable only when used with very fresh rocks. Although the levels of strontium in the Slide Mountain Group are not inconsistent with the 135 - 300 ppm average for ocean-floor basalts and tholeiites (HART *et al.*, 1970) the Ti-Zr-Y method was chosen as being more certain than the Ti-Zr-Sr method.

Barium is found mainly in feldspars, and a bit in apatite. Like Sr it is concentrated in the oligoclase-labradorite phase, up to 400 ppm (PRINZ, 1967). The average for the rocks of this study is about 65 ppm which is not inconsistent with the values of HART *et al.* (1970). Some samples contain great amounts of Ba however, and this is almost certainly present as sulphate mineralisation.

Transition metals:

Scandium is concentrated in pyroxenes and amphiboles, usually in the Fe sites and occasionally substituting for Mg. The maximum value for basalts is 70 ppm (THOMPSON *et al.*, 1972), a figure which is approached by the komatiites of this study, which average 55 ppm. Scandium values for the tholeiites are quite typical (20-25 ppm) and perhaps a bit below average. In a number of the epidotes studied, Sc is present at a concentration of several hundred ppm, particularly in the more iron-rich epidotes of the komatiite suite.

Vanadium is usually concentrated in magnetite (PRINZ, 1967) and to a lesser degree in pyroxenes. In the Slide Mountain

Group it is primarily present in the pyroxenes and amphiboles, though it is not absent in the oxide phase. Like Sc, it is present in the komatiites in amounts approaching the maximum for basaltic rocks, which in the case of vanadium is 600 ppm (THOMPSON *et al.*, 1972). The average of 350 ppm for the rocks of this study is quite normal. Microprobe studies have shown V to be present at concentrations of 300 - 400 ppm in a number of minerals, reflecting the general lack of an oxide phase in most of these rocks.

Chromium is concentrated in early phase pyroxenes, and particularly prefers augite. These early pyroxenes accept a great deal of Cr and thus preempt the crystallisation of Cr - spinels (PRINZ, 1967). As the magma is depleted in Cr, later pyroxenes are lower in Cr than earlier ones. The amount of Cr in the komatiites is not far above the 550 ppm maximum for basaltic rocks cited by THOMPSON *et al.*, (1972), which suggests that the role played by augite was limited. This casts some doubt on the possible ankaramitic origin of the komatiites of Figure 12. From the higher values of the komatiite suite down to about 200 ppm, the range of Cr values in this study is broad (see Figure 13). If this is not a reflection of Cr depletion of the magma, then it possibly reflects a mantle inhomogeneity (MERCY and O'HARA, 1967) over the large distances between the field areas of this study.

Co-Ni-Cu-Zn:

Cobalt is primarily a trace element of olivines, though some is also found occupying the Fe and Mg sites in pyroxenes and amphiboles. It decreases gradually with differentiation, and it is

present in concentration usually under 80 ppm in basalts (THOMPSON *et al.*, 1972). Average values of 85-95 ppm in this study almost certainly are a result of contamination from the tungsten carbide swing mill.

Nickel, like cobalt, is mostly an element of olivines, and Ni in pyroxenes falls off very quickly with differentiation. Average values of 50-150 ppm (see Figure 13) are much lower than expected, and this is clearly demonstrated in Figure 22. If the Ni:Mg ratio can be taken, during early stages of fractionation, as reflecting the amount of olivine involved in partial melting it becomes quite useful. The Ni:Mg ratio suggests that the Slide Mountain Group tholeiites probably had only partial involvement of olivine, and the komatiites had very little. This postulated lack of olivine would also suggest that the rocks which plot as komatiites on Figure 12 are indeed komatiites and not picrites or oceanites. Finally, Cr:Ni values of greater than 2 are yet another confirmation of the oceanic character of these rocks (GAST, 1968).

Copper is found in all minerals of basalts, but olivine, pyroxene, and plagioclase are all Cu-rejectors compared to the melt (PRINZ, 1967) and Cu is usually present as chalcopyrite.

Zinc has been shown to be present in minor amounts in many of the minerals of this study, and averages, overall, about 100 ppm in the rocks of the Slide Mountain Group.

Molybdenum and Lead:

Both Mo and Pb are present in amounts under 10 ppm, and the data are not reliable for Pb, giving only magnitude.

Figure 22: Ni vs MgO

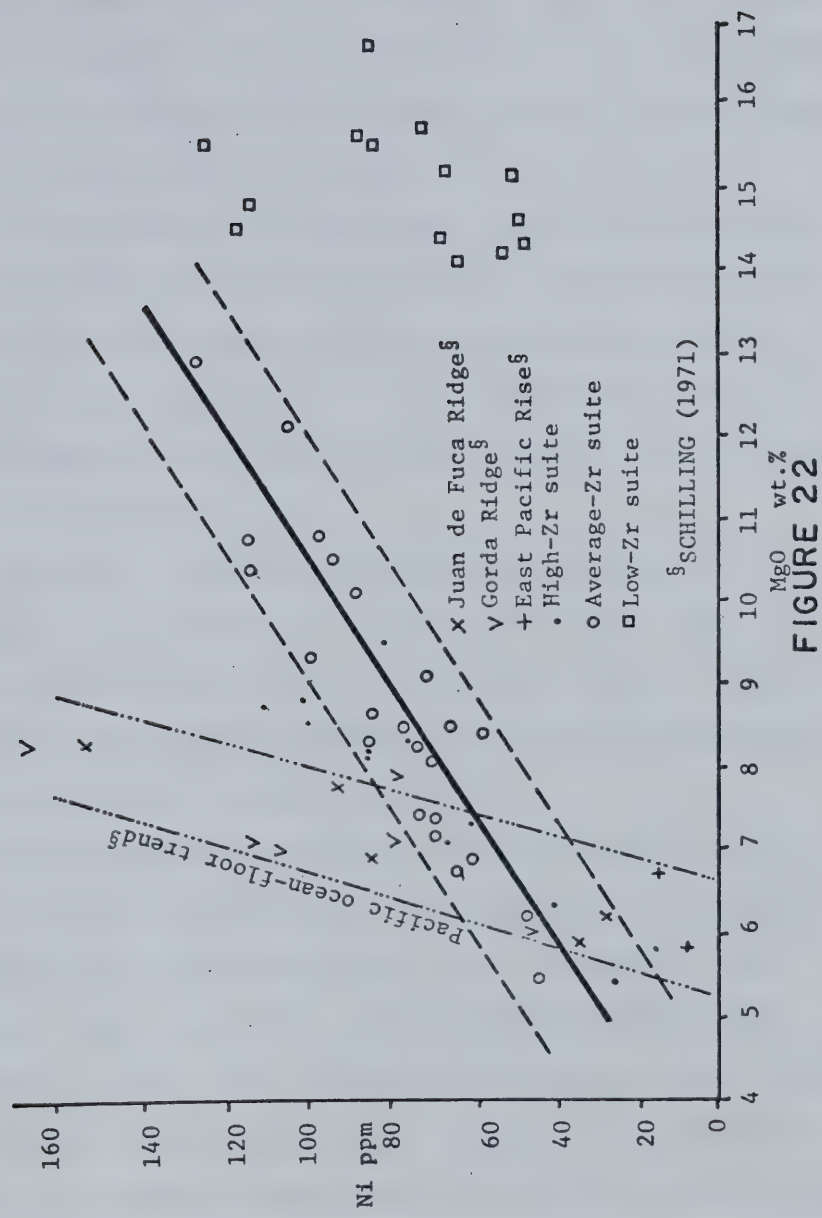


FIGURE 22

CONCLUSION:

The basaltic rocks of the Slide Mountain Group are petrologically highly varied. In the field they range from a coarse-grained amphibolite to fine-grained basalts, and from devitrified glasses to cataclased chlorite schists. Pillow lavas are common, but by no means dominant features.

In thin section, the amphibolites of the MacKay River Map Area comprise a small suite of rocks representing several stages in the progressive hydrous amphibolitisation of a pyroxenite. Most of the other lithologies contain considerable amounts of devitrified glass and exhibit textures similar to basalts dredged from the ocean-floor.

Microprobe studies reveal a probable miscibility gap between the hornblendes and the actinolites of this study, as well as the iron-rich nature of the epidotes present. Plagioclase is of the low-Ca variety in many of the rocks of the Group, but is virtually absent from the amphibolites.

Metamorphism of the Slide Mountain Group has been to the very lowest greenschist facies, with pumpellyite sometimes present. Chlorite and actinolite are common to all the basaltic rocks studied. The interpretation of the metamorphic events which produced the amphibolites in the MacKay River Map Area is limited by both poor exposure and paucity of samples. Rocks to the south have reached the amphibolite facies, but indications in the MacKay River Map Area are that metamorphism there was also to the lowest greenschist facies.

In spite of the metamorphic overprint, there is a strong impression given by the textures, the presence of pillow lavas, etc, that the suite of rocks from this study is a suite of ocean-floor material. Chemically, the ocean-floor nature of the rocks has been conclusively established using several chemical screens. Most of the rocks are tholeiites, and the tendency towards low potash values in most samples points strongly to their oceanic origin. This is further confirmed by the use of a $\text{TiO}_2 - \text{K}_2\text{O} - \text{P}_2\text{O}_5$ diagram. Further, the potash values indicate that the rocks are associated with the generation of ocean-floor material rather than with the generation of island arc material.

A number of the rocks studied have komatiitic chemical compositions (affinities). Elemental migration has been ruled out, and the composition is taken as being primary. On a $\text{CaO} - \text{MgO} - \text{Al}_2\text{O}_3$ diagram most of the komatiitic rocks plot in the vicinity of the Badplaas type. Many correspond with an overlapping field for picrites and ankaramites which projects onto the diagram, but low Ni and Cr concentrations seem to rule out that possibility.

The chemical relationships of Y and Ca are consistent with a model for production of tholeiite by the fractionation of garnet peridotite. The relationships also suggest that the komatiitic rocks are the product of orthopyroxene - clinopyroxene fractionation with minor olivine involvement. Zirconium distribution highlights the difference between the komatiitic suite and the tholeiitic suite. In conjunction with Y and Ti, Zr provides another confirmation of the ocean-floor origin of the suite as a

whole. Another confirmation of the ocean-floor of the rocks of this study is the Cr:Ni ratio.

In summary, major and trace element studies confirm the ocean-floor origin of the Slide Mountain Group, making it the first reported ocean-floor basalt in the Cordillera. The suite is further divided into a group of tholeiites and a smaller group komatiitic rocks on the basis of bulk chemistry. Although there are some difficulties with the development of a suitable chemical screen for komatiites, the komatiitic rocks of this study are the youngest known examples in North America, at least, and the first reported from the Cordillera. Once thought to be the product of peculiar Archaean conditions, komatiites might be better viewed as a normal, though rare, aspect of mantle-lithosphere interaction.

Higher degrees of partial melting tend to produce peridotite and peridotitic komatiites. Very rapid rise of mantle material would tend to leave the olivine component behind, and whether peridotites (common) or komatiites (uncommon) are produced would seem to be dependent not so much upon the origin as on the rate of ascent of material from a level of the mantle deeper than that which evolves into the mass of oceanic tholeiites.

This study of the Slide Mountain Group is an introductory one. Much additional work should be done on these rocks and on those (possibly equivalent) of the Cache Creek Group before the model of their tectonic and chemical evolution can be more than a paradigm.

REFERENCES CITED

- AL'MUKHADEMOV, AI (1967) Behavior of Titanium during differentiation of basaltic magma. *Geochem. Int.* 4, 47
- AUMENTO, F (1972) The crust of the mid-atlantic ridge at 45°N. *in* The Ancient Oceanic Lithosphere; Publ. Earth Phys. Branch, EMR, 42, 49 Ottawa
- AUMENTO, F; LONCAREVIC, BD; and ROSS, DI (1971) Hudson Geotraverse: geology of the mid-atlantic ridge at 45°N. *Phil. Trans. Roy. Soc. Lond.* A268, 623
- BAILEY, EH and BLAKE, MC (1974) Major chemical characteristics of mesozoic Coast Range ophiolite in California. *Jour. Research USGS* 2, 637
- BICKLE, MJ and NISBET, E (1972) The oceanic affinities of some alpine mafic rocks based on their Ti-Zr-Y contents. *Jour. Geol. Soc.* 128, 267
- BROOKS, C and HART, S (1972) An extrusive basaltic komatiite from a Canadian Archaean metavolcanic belt. *Can. Jour. Earth Sci.* 9, 1250
- BROOKS, C and HART, S (1974) On the significance of komatiite. *Geology* 2, 107
- CAMPBELL, KV (1971) Metamorphic petrology of the Crooked Lake area, Cariboo Mountains, British Columbia. Ph.D thesis University of Washington
- CAMPBELL, RB and TIPPER, HW (1971) Geology of the Bonaparte Lake map area, British Columbia. *Geol. Surv. Canada Memoir* 363
- CANN, JR (1970) Rb, Sr, Y, Zr, and Nb in some ocean floor basaltic rocks. *Earth Plan. Sci. Lett.* 10, 7
- CANN, JR (1971) Major element variations in ocean floor basalts. *Phil. Trans. Roy. Soc. Lond.* A268, 495
- CAWTHORN, RG and STRONG, DF (1974) The petrogenesis of komatiites and related rocks as evidence for a layered upper mantle. *Earth Plan. Sci. Lett.* 23, 369
- CHURCH, WR (1972) Ophiolite: its definition, origin as oceanic crust, and mode of emplacement in orogenic belts. *in* The Ancient Oceanic Lithosphere; Publ. Earth Phys. Branch, EMR, 42, 71 Ottawa
- CLARKE, DB (1970) Tertiary basalts of Baffin Bay: possible primary magma from the mantle. *Cont. Min. Petr.* 25, 203
- ENGEL, AEJ; ENGEL, CG; and HAVENS, RG (1965) Chemical characteristics of oceanic basalts and the upper mantle. *Bull. Geol. Soc. Am.* 76, 719

- ERNST, WG (1968) Amphiboles
Springer-Verlag, New York
- FLANAGAN, FJ (1973) 1972 values for international geochemical reference samples. *Geoch. et Cosmoch. Acta* 37, 1189
- FOSCOLOS, AE and BAREFOOT, RR (1970) A buffering and standard addition technique as an aid in the comprehensive analysis of silicates by atomic absorption spectroscopy. *Geol. Surv. Canada Paper* 70-16
- GALE, GH (1973) Paleozoic basaltic komatiite and ocean-floor type basalts from northeastern Newfoundland. *Earth Plan. Sci. Lett.* 18, 22
- GAST, PW (1968) Trace element fractionation and origin of tholeiite and alkaline magma types. *Geoch. et Cosmoch. Acta* 32, 1057
- HARRIS, WE and KRATOCHVIL, B (1974) Chemical Separations and Measurements WB Saunders Co. Toronto
- HART, SR (1970) Chemical exchange between sea water and deep ocean basalts. *Earth Plan. Sci. Lett.* 9, 269
- HART, SR (1971) K, Rb, Cs, Sr, and Ba contents and Sr isotope ratios of ocean floor basalts. *Phil. Trans. Roy. Soc. Lond.* A268, 573
- HART, SR; *et al.* (1970) Ancient and modern volcanic rocks: a trace element model. *Earth Plan. Sci. Lett.* 10, 17
- HASHIMOTO, M (1972) Reactions producing actinolite in basic metamorphic rocks. *Lithos* 5, 19
- JAMIESON, BG and CLARKE, DB (1970) Potassium and associated elements in tholeiitic basalts. *Jour. Petr.* 11, 183
- KAY, R; HUBBARD, NJ; and GAST, PW (1970) Chemical characteristics and origin of oceanic ridge volcanic rocks. *Jour. Geophys. Res.* 75, 1585
- KUNO, H (1967) Differentiation of basalt magmas. *in Basalts* Hess, HH and Poldervaart, A (eds.) p.623 Interscience, New York
- LAMBERT, RStJ and HOLLAND, JG (1974) Yttrium geochemistry applied to petrogenesis utilizing calcium-yttrium relationships in minerals and rocks. *Geoch. et Cosmoch. Acta* 38, 1393
- MANSON, V (1967) Geochemistry of basaltic rocks: major elements. *in Basalts* Hess, HH and Poldervaart, A (eds.) p.215
- MERCY, E and O'HARA, MJ (1967) Distribution of Mn, Cr, Ti, and Ni in coexisting minerals of ultramafic rocks. *Geoch. et Cosmoch. Acta* 31, 2331

- MIYASHIRO, AF; SHIDO, F; and EWING, M (1969) Diversity and origin of abyssal tholeiite from the mid-Atlantic ridge near 24° and 30° north latitude. *Cont. Min. Petr.* 23, 38
- MIYASHIRO, AF; SHIDO, F; and EWING, M (1970) Crystallization and differentiation in abyssal tholeiites and gabbros from mid-ocean ridges. *Earth Plan. Sci. Lett.* 7, 361
- MONGER, JWH (1972) Oceanic crust in teh Canadian cordillera. *in* The Ancient Oceanic Lithosphere; Publ. Earth Phys. Branch, EMR, 42, 55 Ottawa
- MONGER, JWH; SOUTHER, JG; and GABRIELSE, H (1972) Evolution of the Canadian cordillera: a plate tectonic model. *Am. Jour. Sci.* 272, 577
- MOORES, EM (1969) Petrology and structure of teh Vourinos ophiolitic complex of northern Greece. *Geol. Soc. Am. Spec. Paper* 118
- PEARCE, JA; and CANN, JR (1971) Ophiolite origin investigated by discriminant analysis using Ti, Zr, and Y. *Earth Plan. Sci. Lett.* 12, 339
- PEARCE, JA; and CANN, JR (1973) Tectonic setting of basic volcanic rocks determined using trace element analyses. *Earth Plan. Sci. Lett.* 19, 290
- PEARCE, JA; GORMAN, BE; and BIRKETT, TC (1975) The TiO_2 - K_2O - P_2O_5 diagram: a method of discrimination between oceanic and non-oceanic basalts. *Earth Plan. Sci. Lett.* 24, 419
- PRINZ, M (1967) Geochemistry of basaltic rocks: trace elements. *in* Basalts Hess, HH and Poldervaart, A (eds.) p.271
- RIDLEY, WI; *et al.* (1974) Basalts from Leg 6 of the Deep Sea Drilling Project. *Jour. Petr.* 15, 140
- SCHILLING, J-G (1971) Sea-floor evolution: rare earth evidence. *Phil. Trans. Roy. Soc. Lond.* A268, 663
- SEKI, Y (1969) Facies series in low grade metamorphism. *Jour. Geol. Soc. Japan* 75, 255
- SHIDO, F; and MIYASHIRO, A (1959) Hornblende of basic metamorphic rocks. *Jour. Fac. Sci. Univ. Tokyo II*, 12, 85
- SHIDO, F; MIYASHIRO, A; and EWING, M (1971) Crystallization of abyssal tholeiites. *Cont. Min. Petr.* 31, 251
- SIGHINOLFI, GP (1971) Investigation into deep crustal levels: fractionating effects and geochemical trends related to high grade metamorphism. *Geoch. Cosmoch. Acta* 35, 1005
- SMITH, RE (1968) Redistribution of major elements in the alteration of some basic lavas during burial metamorphism. *J. Pet.* 9, 191
- SMITHERINGALE, WG (1972) Low-potash Lush's Bight tholeiites: ancient oceanic crust in Newfoundland? *Can. J. Ear. Sci.* 9, 574

- SOUTHER, JG (1972) Mesozoic and Tertiary volcanism of the western Canadian cordillera. *in* The Ancient Oceanic Lithosphere; Publ. Earth Phys. Branch, EMR, 42, 55 Ottawa
- SPRINGER, RK (1974) Contact metamorphosed ultramafic rocks in the western Sierra Nevada foothills, California. *Jour. Petr.* 15, 160
- THOMPSON, G; SHIDO, F; and MIYASHIRO, A (1972) Trace element distributions in fractionated oceanic basalts. *Chem. Geol.* 9, 89
- TUREKIAN, KK (1963) The Cr and Ni distribution in basaltic rocks and eclogites. *Geoch. et Cosmoch. Acta* 27, 835
- UPADHYAY, HD; *et al.* (1971) The Betts Cove ophiolite complex, Newfoundland: Appalachian oceanic crust and mantle. *Geol. Assoc. Canada Proceedings* 24, 27
- VILJOEN, MJ and VILJOEN, RP (1969a) The geology and geochemistry of the lower ultramafic unit of the Onverwacht Group and a proposed new class of igneous rocks. *Geol. Soc. S. Afr. Spec. Pub. 2* (Upper Mantle Project) p.55
- VILJOEN, MJ and VILJOEN, RP (1969b) Evidence for the existence of a mobile extrusive peridotitic magma from the Komati Formation of the Onverwacht Group. *Geol. Soc. S. Afr. Spec. Pub. 2* (Upper Mantle Project) p.87
- VILJOEN, MJ and VILJOEN, RP (1970) Archaean vulcanicity and continental evolution in the Barberton region, Transvaal. *in* African Magmatism and Tectonics Clifford and Gass (eds.) [a volume in honour of WQ Kennedy] Oliver & Boyd, Edinburgh p.27
- WELCHER, FJ (1963) Standard Methods of Chemical Analysis (6th ed.) vol 2 p 2267 Van Nostrand, Toronto
- WILKINSON, JFG (1967) The petrography of basaltic rocks. *in* Basalts Hess, HH and Poldervaart, A (eds.) p 163
- YODER, HS and TILLEY, CE (1962) Origin of basalt magmas: an experimental study of natural and synthetic rock systems. *Jour. Petr.* 3, 342

APPENDIX 1: ANALYTICAL PROCEDURES

Atomic Absorption Spectrophotometry:

The elements Li, Sc, V, Cr, Co, Ni, Cu, Mo, and Pb were analysed on a Perkin-Elmer "503" using the following method.

- Rock powders were weighed out at $1,0000 \pm 0,0001$ g and leached with 10 mL concentrated HF and 10 mL concentrated HNO_3 .
- After evaporating to dryness, the dissolution was repeated.
- Samples were moistened, dissolved in 20 mL concentrated HNO_3 , and evaporated to dryness. This was repeated five times to remove fluorine by destroying CaF_2 .
- Samples were moistened and 1 mL concentrated HNO_3 added. About 50 mL water was added and the solution allowed to evaporate to 15 mL.
- This solution was filtered as necessary, and diluted to $25,00 \pm 0,01$ mL and transferred to stoppered bottle.

Accuracy and precision were determined as follows.

- Ten splits were analysed for precision of technique.
- A blank was determined, particularly to evaluate Cr and Pb contamination from the acids and Pb contamination from the air.
- Accuracy was determined using addition dilution (FOSCOLOS and BAREFOOT, 1970).
- USGS Standard basalt [BCR-1] and Standard peridotite [PCC-1] were analysed for comparison to published values (FLANAGAN, 1973).
- These results were summarised as a margin of reasonable certainty and applied to the results in the table which follows.

TABLE A-1: ANALYSED STANDARDS

Element	[BCR-1]* publ.	[BCR-1]	[PCC-1]* publ.	[PCC-1]	Margin [¶]
Li	<u>12,8</u>	12,8	2	2,7	2%
Sc	33	31	6,9	7	5%
V	399	420	30	30	3%
Cr	17,6	19	-	nd	5%
Co	-	nd	112	110	15%
Ni	15,8	16	-	nd	3%
Cu	18,4	18,3	11,3	12	3%
Mo	1,1	3	0,2	2	20%
Pb	17,6	20	13,3	20	50%

* FLANAGAN (1973)

12,8 Recommended value

16 Average value

33 Order of magnitude

[¶] Let us use, as an example of how the margin of uncertainty is obtained, the element Li. The ten splits of [5608] have a mean value of 14,56 ppm Li. This can be used to calculate the precision as follows. The best estimate of standard deviation, σ_1 , is made using the usual formula

$$\sigma_1 = \sqrt{\sum [x_i - \bar{x}]^2 / (n-1)}$$

and in the case of Li for this sample, $\sigma_1 = 0,0685$. Because the number of splits analysed was low, there is some uncertainty in the value σ_1 itself. This sample standard deviation, σ_2 , (or if you will, the uncertainty of the uncertainty) can be calculated to the 95% confidence level using the equation

$$\sigma_2 = \sigma_1 / (\sqrt{2(n-1)}) (0,5)$$

which yields $\sigma_2 = 0,0326$. Assuming that the σ_2 is at its most unfavourable extreme for precision, σ_1 can be as much as 0,101. Thus the concentration of Li in [5608] is 14,56 \pm 0,10 ppm, precise

to $\pm 0,64\%$.

In calculating accuracy by addition dilution, three more splits of [5608] were prepared, and to them was added during the procedure 5, 10, and 15 ppm Li. This gave analysed results of 19,5 ppm 24,4 ppm and 29,5 ppm respectively, and once the additions were subtracted, the mean value of the samples was found to be 14,46 ppm. The best estimate of standard deviation, σ_3 , is 0,083. Since there were only three samples, the sample standard deviation, σ_4 (95%), is horrendous. The $\sigma_4=0,083$, and thus the most unfavourable $\sigma_3=0,166$. Consequently, Li in [5608] is taken as being $14,46 \pm 0,166$ ppm. The accuracy of the method, therefore is $\pm 1,14\%$.

Applying the concept of least favourable combination of uncertainties once again, the two percentages for precision and accuracy are added, giving an overall uncertainty for the procedure of $\pm 1,78\%$, rounded to the 2% margin quoted for Li.

Permanganometric Titration of Ferrous Iron:

Ferrous iron was determined after the method of HARRIS and KRATOCHVIL (1974) with some modifications (WELCHER, 1963).

- Potassium permanganate solution was prepared, aged, and standardised with sodium oxalate to 0,020 M.
- Rock samples were carefully crushed and hand ground under acetone to pass 0,2 mm.
- Samples weighing $0,5000 \pm 0,0001$ g were dissolved under CO_2 in concentrated HF and H_2SO_4 , then held at 95°C for fifteen minutes under CO_2 .
- They were then flooded with cold, recently boiled water through which had been bubbled CO_2 .
- Zimmerman Reinhardt Reagent ($\text{MnSO}_4 + \text{H}_2\text{SO}_4 + \text{H}_3\text{PO}_4$) was added to control the speed of reaction with the titrant, and the sample was titrated slowly with permanganate solution until the pink colour remained for thirty seconds.
- The amount of ferrous iron was calculated and reported.

The samples for which FeO was directly determined show their iron values with asterisks. Total iron was determined for the entire suite of Slide Mountain Group rocks and reported as Fe_2O_3 by xray fluorescence, and this was felt to be unsatisfactory. The Fe_2O_3 (XRF) values of several of the titrimetrically determined samples were converted to oxygen-free values as a crosscheck. The iron in these samples was reduced to ferrous iron and titrated using the above procedure to determine total iron. In all cases,

agreement with xray values was excellent.

Oxidation ratios ($100[\text{Fe}_2\text{O}_3/\text{Fe}_2\text{O}_3+\text{FeO}]$) were calculated and range from 21% to 32% with an average of 27%. These ratios are in very good agreement with several results of Geological Survey of Canada determinations reported by KV CAMPBELL (1971) for rocks from the same locales. This 27% oxidation ratio has been applied to all the xray total iron results and reported as Fe_2O_3 and FeO in the body of this thesis.

Determination of Carbonate:

The carbon content of fifteen samples was determined by combustion using the "LECO" Carbon Determinator, Model 761-100.

In brief, the determinator detects the difference in thermal conductivity between two gases. The cell consists of a pair of thermistors used in two legs of a Wheatstone bridge. The 'reference' thermistor is kept in gas of constant pressure, temperature, and composition, whilst the 'measure' thermistor is located in a cell in which the gas composition varies.

The introduction of CO_2 from the combustion of carbon will cause the temperature of the 'measure' thermistor to increase because the thermal conductivity of CO_2 is lower than that of the reference gas (O_2). Hence the bridge becomes unbalanced and a quantitative output is available to the electronics. This determination of C is accurate $\pm 0.001\%$.

These values were then converted to CO_2 values and a working curve prepared for quick acid determination. The remaining samples were then analysed for CO_2 on the basis of response to acid, and are accurate to $\pm 0.1\%$.

Electron Microprobe:

A number of minerals were analysed for major and trace elements using an ARL-EMX microprobe set up for energy dispersive analysis using an ORTEC Si(Li) detector and accompanying electronics at 15 kV and 0,300 microamps beam current. The counting time was corrected for integrated probe current and the data reduced using the "EDATA" program at the University of Alberta Computer Centre.

Standards:

Kakanui Kaersutite	Mg, Si, Ca, Mn
Hohenfels Sanidine	Al, K
Stillwater Chromite	V, Cr, Co, Ni
Odergarden Ilmenite	Sc, Ti, Fe
Durango Fluorapatite	F,* P, Cl
Albite (Clevelandite)	Na

* analysed semi-quantitatively using
wavelength dispersive analysis

Xray Fluorescence:

Whole rock powders were ground to 0,05 mm, compressed into pellets, and analysed on a Phillips 1212 machine using major international standards for major elements and spiked Pilkington glasses for trace elements.

All analyses were accomplished at Durham University under the direction of J. Grenville Holland.

TiO₂ analyses from this lab tend to be a bit high.

APPENDIX 2: CIPW NORMS AND OTHER VALUES

CIPW norms were calculated using the computer program *CIPWNORM*, an APL program in the University of Alberta Computer Centre users' library. The same program was also used to compute the alkali ratio $[K_2O/Na_2O+K_2O]$, the Thornton Tuttle Differentiation Index, and the values used in Figure 11.

TABLE A-2a: CIPW NORMS OF HIGH-ZR SUITE

	[5550S]	[5551X]	[5551Y]	[5551Z]	[5552A]
Q	0	0,4	0	0	0,7
Or	0,7	0,7	3,2	1,2	1,6
Ab	35,5	24,6	28,4	32,8	24,8
An	21,6	20,7	26,5	18,1	25,7
Di	14,5	24,0	10,0	19,3	12,9
Hy	7,7	19,4	13,7	14,3	22,9
Ol	11,4	0	9,5	4,0	0
Mt	4,6	4,8	4,6	4,5	4,6
Il	3,4	3,4	3,2	3,7	3,2
Py	0,1	0,3	0,2	1,3	0,1
Ap	0,4	0,4	0,5	0,4	0,4
Cc	0	1,4	0	0,2	0
K/Na+K	0,03	0,03	0,14	0,05	0,09
Diff.*	36	26	32	34	30
	[5552B]	[5552Z]	[5553A]	[5553B]	[5553C]
Q	1,5	0	0	0	1,0
Or	1,1	0,5	2,0	0,3	0,4
Ab	32,8	16,8	22,8	18,1	28,1
An	22,2	26,9	27,8	26,3	24,6
Di	10,8	27,7	14,9	29,5	13,9
Hy	23,4	16,6	18,7	13,7	23,5
Ol	0	2,4	4,8	3,0	0
Mt	4,4	4,9	4,9	4,8	4,7
Il	3,2	3,3	3,3	3,3	3,1
Py	0,1	0,2	0,3	0,4	0,2
Ap	0,4	0,5	0,5	0,5	0,4
Cc	0	0	0	0	0
K/Na+K	0,05	0,05	0,11	0,02	0,02
Diff.*	35	17	25	18	30

* Thornton Tuttle Differentiation Index

TABLE A-2b: CIPW NORMS OF HIGH-ZR SUITE

	[5553Y]	[5553Z]	[5554A]	[5554B]	[5555]
Q	1,0	0	2,2	4,4	0
Or	0,7	1,6	0,8	0,8	3,9
Ab	21,3	26,7	26,5	26,1	30,2 +
An	24,7	24,2	27,7	25,7	20,3
Di	24,3	15,7	9,7	12,2	25,9
Hy	19,2	14,0	24,2	22,1	0
Ol	0	8,6	0	0	11,0
Mt	4,7	5,1	4,8	4,7	4,3
Il	3,2	3,4	3,3	3,3	3,1
Py	0,4	0,3	0,4	0,2	0,3
Ap	0,4	0,4	0,5	0,5	0,4
Cc	0,2	0	0	0	0
K/Na+K	0,04	0,08	0,04	0,04	0,15
Diff.*	23	28	30	31	35
	[5556A]	[5556B]	[5556Y]	[5556Z]	[5558A]
Q	4,2	1,5	0	0	0
Or	0,3	0,4	0,6	0,6	2,2
Ab	25,5	21,9	25,3	35,8	32,5
An	26,5	28,6	26,3	21,6	21,4
Di	12,3	13,8	17,4	14,7	16,1
Hy	23,6	24,8	10,7	6,4	11,9
Ol	0	0	11,4	12,3	7,5
Mt	4,5	4,8	4,2	4,7	4,6
Il	3,2	3,3	3,3	3,5	3,3
Py	0,3	0,2	0,4	0,1	0,1
Ap	0,4	0,5	0,4	0,5	0,4
Cc	0	0	0	0	0
K/Na+K	0,02	0,03	0,03	0,02	0,09
Diff.*	29	24	26	36	35

* Thornton Tuttle Differentiation Index + also Ne 0,6

TABLE A-2c: CIPW NORMS OF HIGH-ZR SUITE

	[5607]	[5613A]	[5614]	[5621]
Q	5,6	0	0	3,5
Or	0,9	0,5	1,0	3,6
Ab	38,1	31,0	25,5	37,2
An	17,8	20,0	22,3	18,9
Di	13,6	22,3	20,7	12,7
Hy	15,6	6,7	15,7	16,0
Ol	0	9,3	3,1	4,0
Mt	3,8	5,1	5,0	4,0
Il	3,5	3,9	4,2	3,6
Py	0,3	0,5	1,3	0
Ap	0,7	0,5	0,4	0,5
Cc	0	0,2	0,8	0
K/Na+K	0,03	0,02	0,05	0,12
Diff*	45	32	26	44
	[5636]	[5636B]	[5636C]	
Q	0	1,8	0	
Or	0,2	1,6	0,2	
Ab	25,5	21,4	27,8	
An	26,1	28,6	24,2	
Di	17,7	15,3	18,0	
Hy	11,4	21,7	9,6	
Ol	9,2	0	9,9	
Mt	5,6	5,0	5,1	
Il	3,6	3,7	4,1	
Py	0	0,2	0,2	
Ap	0,6	0,5	0,6	
Cc	0	0,2	0,2	
K/Na+K	0,01	0,09	0,01	
Diff.*	26	25	28	

* Thornton Tuttle Differentiation Index

TABLE A-3a: CIPW NORMS OF AVERAGE-ZR SUITE

	[5550R]	[5550T]	[5550U]	[5550V]	[5550W]
Q	0	0	0	0	0
Or	0,2	0,3	0,4	0,8	0,1
Ab	26,4	10,5 +	33,1	29,3	33,4
An	23,6	26,6	18,2	21,5	20,5
Di	28,5	39,0	30,1	29,5	26,2
Hy	3,8	0	5,1	7,7	3,7
Ol	8,9	8,9	5,0	3,4	8,1
Mt	4,8	5,5	4,2	4,2	3,7
Il	3,2	4,2	3,1	3,3	3,5
Py	0	0,3	0,2	0	0,4
Ap	0,5	0,5	0,3	0,4	0,4
Cc	0,1	0	0,2	0	0
K/Na+K	0,01	0,02	0,02	0,04	0,01
Diff.*	27	15	33	30	33
	[5550X]	[5550Y]	[5550Z]	[5557]	[5557Z]
Q	0	0	0	0	0
Or	0,5	0,7	0,5	0,2	0,8
Ab	36,9	19,6	31,4	26,4	29,9
An	20,0	28,4	23,6	25,0	22,5
Di	23,7	21,8	18,6	15,1	18,8
Hy	8,7	4,0	6,4	17,4	14,3
Ol	1,6	14,9	10,8	5,4	5,2
Mt	4,0	5,9	4,8	4,8	4,2
Il	3,0	3,6	3,3	3,5	3,4
Py	0,6	0,1	0,1	0,3	0,4
Ap	0,4	0,4	0,4	0,4	0,4
Cc	0,5	0,7	0	1,4	0,2
K/Na+K	0,02	0,05	0,02	0,01	0,04
Diff.*	37	20	32	27	31

* Thornton Tuttle Differentiation Index + also Ne 4,3

TABLE A-3b: CIPW NORMS OF AVERAGE-ZR SUITE

	[5558B]	[5558Z]	[5602]	[5603]	[5606]
Q	0	0	5,9	6,3	0
Or	0	3,4	0,4	0	13,4
Ab	40,9	9,3	23,0	4,3	18,0
An	19,9	28,2	24,5	24,4	22,9
Di	14,9	25,0	25,8	57,0	15,2
Hy	5,3	0,5	12,5	0	10,1
Ol	11,1	23,2	0	0	10,0
Mt	4,2	6,0	4,3	4,4	4,7
Il	3,1	3,6	3,1	2,6	3,5
Py	0,4	0,4	0,3	0,6	0,3
Ap	0,4	0,4	0,3	0,3	0,4
Cc	0	0	0	0	1,4
K/Na+K	0,00	0,34	0,02	0,00	0,52
Diff.*	41	13	29	11	31

	[5608]	[5610]	[5610A]	[5611B]	[5611C]
Q	0	0	0	0	0
Or	0,8	1,5	1,2	4,5	3,2
Ab	24,8	31,3	27,4	35,1	36,7
An	26,4	26,1	27,5	18,2	19,7
Di	21,5	2,9	12,4	12,4	7,2
Hy	5,1	16,2	15,1	15,1	15,6
Ol	14,3	13,9	6,0	5,1	17,2
Mt	3,3	4,6	4,5	4,2	4,4
Il	2,7	3,9	3,3	3,1	3,5
Py	0,4	0,2	0,3	0,2	1,5
Ap	0,5	0,3	0,3	0,3	0,3
Cc	0	0	0,2	0	0,7
K/Na+K	0,05	0,06	0,06	0,16	0,11
Diff.*	26	33	29	40	40

* Thornton Tuttle Differentiation Index

TABLE A-3c: CIPW NORMS OF AVERAGE-ZR SUITE

	[5615]	[5616]	[5617]	[5618]	[5619]
Q	0	0	1,1	0	0
Or	3,3	3,1	2,9	2,3	3,9
Ab	23,1	5,2	31,1	22,0	29,4
An	27,9	29,6	18,4	26,3	22,7
Di	11,1	38,0	20,0	17,7	15,1
Hy	11,6	3,7	18,1	11,1	9,7
Ol	13,7	11,5	0	12,5	10,5
Mt	5,5	5,2	4,2	4,6	4,7
Il	2,8	3,1	3,5	3,0	3,3
Py	0,1	0	0,3	0	0,3
Ap	0,3	0,4	0,4	0,5	0,4
Cc	0,6	0,2	0	0	0
K/Na+K	0,17	0,46	0,12	0,13	0,16
Diff.*	26	8	35	24	33

	[5619A]	[5620]	[5630]	[5630B]
Q	0	0	0	0
Or	0,4	0,4	1,0	0,6
Ab	37,7	20,4	18,4	26,9
An	20,0	23,5	26,7	24,0
Di	15,9	25,2	17,9	15,6
Hy	9,2	17,5	17,3	16,8
Ol	8,9	3,3	10,4	8,2
Mt	4,1	4,9	5,2	4,4
Il	3,3	3,1	2,3	2,6
Py	0,2	0	0	0,4
Ap	0,4	0,5	0,5	0,5
Cc	0	1,4	0,3	0
K/Na+K	0,02	0,02	0,07	0,03
Diff.*	38	21	19	27

* Thornton Tuttle Differentiation Index

TABLE A-4a: CIPW NORMS OF LOW-ZR SUITE

	[5720]	[5720A]	[5721]	[5721A]	[5721B]
Q	0	0	0	0	0
Or	3,1	2,8	1,5	0,9	0,8
Ab	5,1	2,0	4,9	3,7	0,3
An	11,9	14,2	13,1	17,7	20,0
Di	41,4	39,7	40,1	43,1	42,2
Hy	13,9	22,7	18,3	14,1	25,9
Ol	14,9	9,8	11,1	10,7	3,7
Mt	7,0	6,3	7,7	6,6	5,2
Il	2,4	2,3	2,0	1,6	1,4
Py	0,2	0,1	0	0	0
Ap	0,1	0,2	0,1	0,4	0,6
Cc	0	0	0,2	1,1	0
K/Na+K	0,46	0,67	0,30	0,25	0,81
Diff.*	8	5	6	5	1

	[5722B]	[5722C]	[5724]	[5725]	[5725A]
Q	0	0	0	0	0
Or	0,7	1,0	0,5	0,4	0,5
Ab	0,7	0,9	4,5	3,2	0
An	17,6	20,9	12,7	28,2	32,5
Di	46,3	42,1	45,7	16,7	9,2
Hy	10,1	12,6	2,2	1,7	25,7
Ol	14,9	14,0	25,4	37,9	21,9
Mt	6,6	6,1	6,6	8,5	7,6
Il	2,3	2,1	2,1	1,7	1,7
Py	0,1	0	0	0	0
Ap	0,8	0,3	0,2	0,9	1,0
Cc	0	0	0	0,7	0
K/Na+K	0,60	0,62	0,15	0,16	1,00
Diff.*	1	2	5	4	0

* Thornton Tuttle Differentiation Index

TABLE A-4b: CIPW NORMS OF LOW-ZR SUITE

	[5726]	[5726A]	[5727]	[5731]
Q	0	0	0	0
Or	1,1	0,7	3,6	0
Ab	3,8	0,3	13,8	33,1
An	19,4	25,9	13,8	29,7
Di	44,2	36,9	28,6	3,2
Hy	5,6	23,4	25,3	17,9
Ol	17,4	5,9	8,6	11,1
Mt	5,9	5,0	4,4	3,5
Il	1,8	1,4	1,2	1,3
Py	0	0	0	0
Ap	0,7	0,5	0,5	0,2
Cc	0	0	0,2	0
K/Na+K	0,30	0,75	0,27	0,00
Diff.*	5	1	17	33

* Thornton Tuttle Differentiation Index

APPENDIX 3: COMPARATIVE TRACE ELEMENT ANALYSES

	[B*]	[C*]	[M*]	[N*]	error # ppm
Li	5,5	45	13,8	6	6
V	488	500	495	480	4
Co	94	56	55	50	6
Ni	148	177	107	250	22
Cu	96	61	54	80	12
Zn	146	152	125	140	6
Rb	10	6	3	19	45
Sr	42	27	30	22	11
Ba	nil@	nil@	nil@	nil@	-
Pb	nilç	nilç	nilç	nilç	-
number	(4)	(2)	(4)	(1)	of data sets

B* from the general area of the Barkerville Map Area

C* from the Crooked Lake area, south of the MacKay River Map Area

M* from the general area of the MacKay River Map Area

N* from the general area of the Clearwater Map Area

error values quoted directly from CAMPBELL's Table 30

All data taken from CAMPBELL (1971)

@ Barium detection limit 30 ppm

ç Lead detection limit 1 ppm

APPENDIX 4: COMPARATIVE CHEMISTRY

Presented in the tables following are fifteen basalt values which are averages of from one to 195 individual analyses. It not a complete selection, and the reader interested in greater detail is referred to MANSON (1967) or ENGEL, ENGEL, and HAVENS (1965) for in depth discussions on tholeiite chemistry; and to BROOKS and HART (1974) for a short, but important discussion of komatiite chemistry and fifteen analyses.

TABLE A-5: COMPARATIVE THOLEIITIC ANALYSES

	[1*]	[2*]	[3*]	[4*]	[5*]
SiO ₂	50,2	49,3	49,4	48,3	47,5
Al ₂ O ₃	16,8	15,2	14,4	14,2	13,8
Fe ₂ O ₃	2,66	3,08	3,3	4,2	3,3
FeO	6,50	7,07	8,2	6,8	6,7
MnO	,14	,39	,17	-	,17
MgO	6,55	7,18	7,8	6,0	11,8
CaO	11,7	9,15	10,5	8,7	11,7
Na ₂ O	2,75	3,22	2,2	3,3	1,53
K ₂ O	,44	,14	,45	,7	,10
TiO ₂	1,40	1,42	2,4	2,2	,97
P ₂ O ₅	,14	,17	,27	-	,10
V	360	348	-	-	-
Cr	125	84	-	-	-
Ni	56	95	-	-	-
Cu	73	150	-	-	133
Zn	99	102	-	-	57
Rb	5	5	-	-	2
Sr	120	195	-	-	161
Y	-	-	-	-	21
Zr	342	116	-	-	66
Ba	94	24	-	-	56

1* AUMENTO (1972)

[10] fresh tholeiites

2* AUMENTO (1972)

[10] metamorphosed tholeiites

3* MANSON (1967)

[195] Pacific Ocean tholeiites

4* BAILEY and BLAKE (1974)

[10] basalts / ophiolite suite

5* CLARKE (1974)

[21] Ol-poor basalts, Baffin Is.

TABLE A-6a: COMPARATIVE KOMATIITIC ANALYSES

	[1ç]	[2ç]	[3ç]	[4ç]	[5ç]
SiO ₂	46,5	42,8	45,1	46,5	46,9
Al ₂ O ₃	7,0	7,3	10,8	8,9	3,64
Fe ₂ O ₃	2,6	2,7	2,4	6,3	1,15
FeO	6,5	8,7	8,1	4,44	9,89
MnO	,18	,17	,18	-	,11
MgO	21,6	25,7	19,7	18,6	20,6
CaO	11,0	6,9	9,2	9,96	16,5
Na ₂ O	,43	1,08	1,04	1,65	,09
K ₂ O	,14	,21	,08	,79	,28
TiO ₂	,25	,97	,76	,51	,89
P ₂ O ₅	,06	,12	,09	,57	-
V	-	-	-	-	-
Cr	-	-	-	-	-
Ni	-	-	-	-	-
Cu	-	77	109	-	-
Zn	-	69	58	-	-
Rb	-	4	2	-	-
Sr	-	191	186	-	-
Y	-	14	18	-	-
Zr	-	67	52	-	-
Ba	-	69	55	-	-
1ç	BAILEY and BLAKE (1974)		[1] amphibolite peridotite		
2ç	CLARKE (1974)		[9] picrites, Svartenhuk		
3ç	CLARKE (1974)		[4] Ol-basalts, Baffin Is.		
4ç	BROOKS and HART (1974)		[1] picrite, New Hebridies		
5ç	BROOKS and HART (1974)		[1] clinopyroxenite, Japan		

TABLE A-6b: COMPARATIVE KOMATIITIC ANALYSES

	[6c]	[7c]	[8c]	[9c]	[10c]
SiO ₂	50,5	48,9	52,8	53,4	53,4
Al ₂ O ₃	5,3	7,55	9,49	9,95	5,54
Fe ₂ O ₃		2,02			
FeO	6,9	11,1	10,7	12,0	10,9
MnO	,12	,02	,17	,22	,22
MgO	20,1	16,7	14,2	10,2	15,5
CaO	16,5	11,4	10,2	10,1	13,1
Na ₂ O	,40	,81	2,00	2,68	1,23
K ₂ O	,01	,07	,12	,46	,09
TiO ₂	,19	1,14	,16	,86	,57
P ₂ O ₅	-	,3	,07	,06	,05
V	-	-	-	-	-
Cr	-	-	1300	-	-
Ni	-	520	330	-	-
Cu	-	-	14	-	-
Zn	-	-	70	-	-
Rb	-	1	<3	-	-
Sr	-	57	136	-	-
Y	-	-	3	-	-
Zr	-	-	14	-	-
Ba	-	-	33	-	-

6c	BROOKS and HART (1974)	[1] Ol-gabbro, Troodos
7c	BROOKS and HART (1972)	[1] pillow lava, Ontario
8c	GALE (1973)	[9] komatiites, Newfoundland
9c	VILJOEN and VILJOEN (1969a)	[3] komatiites, Barberton
10c	VILJOEN and VILJOEN (1969a)	[5] komatiites, Badplaas

B30153